AQUEOUS SLN AND NLC DISPERSIONS

It is known that the incorporation of drug substances into colloidal carriers, such as liposomes and polymeric nanoparticles, can result in improved drug stability and clinical potency, increased drug absorption, and decreased drug toxicity [312-314]. Concerning the development of lipid nanoparticles (SLN and NLC), if they are further optimized in terms of physical properties, the additional advantages of potentially increased solubilization of a poorly soluble drug and thermodynamic stability are realized, from a particle size in the range of 50 to 1000 nm.

The development and the use of SLN and NLC as drug delivery vehicles for antifungals will be the focus of this chapter. However, before proceeding it is important to define the term aqueous SLN or NLC dispersion.

To understand the concept of aqueous dispersion of lipid nanoparticles it is necessary to have some colloidal chemistry background. This system is considered to be based on water, solid lipid and amphiphile molecules that form an opalescent single phase, which needs to be thermodynamically stable. These amphiphile molecules are surfactants that stabilize the aqueous dispersion, which may be described in terms of their hydrophilic and lipophilic nature. It is the balance between these two properties that determines the range of phenomena from surface effects to colloidal behaviour found in these systems. The basic thermodynamic requirement is to reach equilibrium between the minimum free energy and maximum entropy in the system [315]. In fact, the unfavourable entropy consideration associated with the aggregation of amphiphile molecules is balanced by the lower system free energy obtained by maximizing the hydrophilic-water contacts.

Colloidal vehicles have the potential advantages of both improved stability and solubilization characteristics compared to systems in the micrometer range. These advantages are due to the smaller particle size characteristic of the former. It is noteworthy that particles under 1 μm can create translucent (opalescent) systems, providing conceptual appeal to the patient. Furthermore, a homogeneous system also allows to solubilize all of the drugs or other solid materials on the formulation, as well as to obscure the presence of undissolved solids. This is particularly important when the drug is poorly soluble both in the solid lipid and water phase, because bioavailability of a crystalline drug suspension may vary dramatically from that of a solubilized drug. In addition, they have also the property of weaken the coloration of special compounds that can be degraded into products possessing colour. This is a very important

aspect in the development of a new product once appearance is a relevant factor for a dermal product to be purchased and used by the patient, i.e. not only the packaging should be attractive but also the appearance of the product itself.

Many drugs frequently cannot be delivered in pharmacological dose using conventional topical formulations because of insufficient solubility in their components. Therefore, solubilization and/or dispersion of the drug within an aqueous SLN or NLC dispersion may be particularly important.

In order to develop a formulation having properties that are not dependent upon process (i.e. shear forces, induced cooling), and also that the different phases do not separate (temperature and pressure conditions remain reasonably constant), thermodynamic stability needs to be provided.

A thermodynamically stable system means that it state always tends toward to the state having the lowest possible interfacial area [264]. Thus, for an emulsion the thermodynamically stable state is a layer of oil on water, whereas a single particle is the thermodynamically stable state of a suspension. Although all systems tend toward the thermodynamically stable state of minimal interfacial area, which results in dramatic changes in their physicochemical properties, systems may vary considerably in their rate of conversion. As long as the system remains closed (i.e. no evaporation or chemical degradation) and the temperature and pressure remain the same, the properties of the system will remain unchanged indefinitely. However, if the temperature or other thermodynamic parameter responsible for the stability of the system is changed sufficiently to cause drug crystals to precipitate and/or polymorphic transformations in the lipid matrix, then this single phase system transforms into a two phase system following gelation and breaking of the dispersion. Thus, an aqueous SLN or NLC dispersion once in equilibrium will not separate into their component phases provided that the temperature and pressure remain constant. If changes in storage conditions cause the different phases to split, the dispersion will never return to its original thermodynamic, once it is an irreversible process. An additional property of these systems is the controlled release profile that they can exhibit due to the solid core they are composed of. The slower drug diffusion that they can provide is dependent on the morphology of the lipid particles and it is also related to the thermodynamic stability of these systems.

In the present chapter the development, physicochemical characterization, and optimization of imidazole-loaded SLN and NLC formulations are presented. For each imidazole antifungal (clotrimazole and ketoconazole) suitable solid and liquid lipids have been selected according to solubilization properties of both drugs, as well as the melting temperature of the mixtures.

4.1 Development and characterization of clotrimazole-loaded SLN and NLC

Topical formulations containing clotrimazole are well known in the pharmaceutical market. Some commercially available examples are Canesten® cream, Fungizid-Ratiopharm® cream, Gino-Lotremine® and Pan-Fungex® creams. Concerning systems in the nanometer range, this drug has been already entrapped into colloidal carriers, such as liposomes [277, 316, 317]. However, liposomes do not show long-term stability and are of high production costs. The aim of this section is to present a profitable alternative to formulate colloidal carriers for this antifungal agent.

For the present study four different formulations have been developed, two of them containing 1% (m/m) of clotrimazole. Table IV shows their composition (the symbols D116 and Co stand for Dynasan®116 and clotrimazole, respectively). Dynasan®116 has been selected as the solid lipid for clotrimazole entrapment after usual inspection of drug crystals in different melted lipids, based on the light they scatter using a black and white background light box. The selection of Miglyol®812 as liquid lipid for NLC preparation was also based on solubility studies.

Table IV: Composition of Dynasan®116-based SLN and NLC formulations (%, m/m).

Formulation composition	Formulation code			
	D116SLN	D116SLN_Co	D116NLC	D116NLC_Co
Dynasan®116	20.0	19.0	14.0	13.5
Miglyol®812	-	-	6.0	5.5
Tyloxapol®	5.0	5.0	5.0	5.0
Clotrimazole	-	1.0	-	1.0
Water ad	100	100	100	100

For the production of NLC formulations the optimized ratio between Dynasan®116 (solid lipid) and Miglyol®812 (liquid lipid) has been determined after screening different proportions of both lipids by DSC studies to evaluate the absence of free oil in the melted mixtures. No free oil has been detected after running the mixtures of solid and liquid lipids until -50ºC. Mixtures of Dynasan®116 and Miglyol®812 at different ratios have been melted at 85ºC and further analysed by DSC. Fig. 4.1 depicts the melting and the onset temperature

values of bulk Dynasan®116 with increasing amounts of Miglyol®812 from 10% to 40% (m/m).

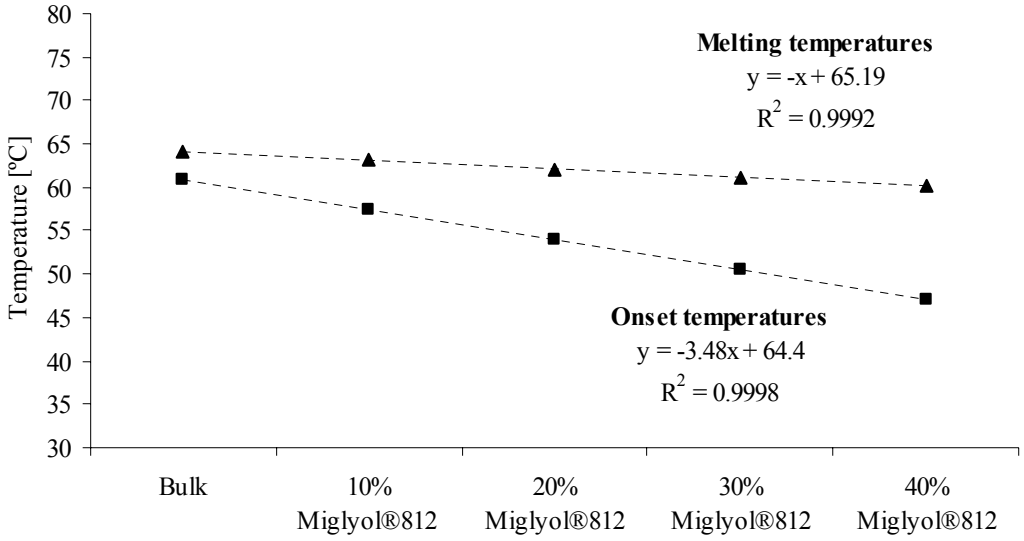

Fig. 4.1: Melting temperature (= peak maximum) and onset temperature values of bulk lipid (Dynasan®116) with increasing amounts of liquid lipid (Miglyol®812) from 10% to 40% (m/m).

The peak maximum of the melting process of pure Dynasan®116 was recorded at 64.21ºC, with an extrapolated onset temperature at 60.98ºC. The difference between the melting and onset temperatures, which is a measure of the width of the melting event, is in this case is 3.23. By adding Miglyol®812 to the bulk lipid, the melting point of the melted mixtures of both lipids is depressed in a concentration dependent manner. With 10% of Miglyol®812 the difference between the temperature values was approximately 5.83 and increased to 13.24 when the mixture had 40% of the same oil. These differences are indicative of the massive crystal order disturbance (lattice defects). The depression of the onset and the temperature of the peak maximum depended on the oil concentration in an approximately linear fashion for the given concentration range (correlation coefficient R^2 = 0.9992 for the melting temperature and R^2 = 0.9998 for the onset temperature). In addition, the slope of the plot of the onset curve (-3.48) was must higher than the slope of the plot for the melting events (-1). A lipid phase containing 30% of Miglyol®812 has been selected once the melting point of the mixture was registered at 61.21ºC with an onset at 50.58ºC. An onset temperature higher than 40ºC is required for lipid colloidal systems intended for topical drug delivery.

4.1.1 Assessment of the physical stability of the developed formulations

It is known that the particle size distribution is one of the most important characteristics for the evaluation of the stability of colloidal systems and also influences the penetration mechanism of drugs into the skin [318, 319]. Therefore, the particle size parameters and the surface electrical charge (zeta potential, ZP) have been evaluated immediately after production of the systems, and during two years of storage at three different temperatures (4ºC, 25ºC and 40ºC).

4.1.1.1 Immediately after production

Under optimized production conditions (500 bar and three homogenization cycles) very small lipid nanoparticles with a negatively charged surface could be obtained. Table V shows the obtained results.

Table V: Zeta potential and particle size parameters of Dynasan®116-based SLN and NLC formulations obtained immediately after production.

Parameters		D116SLN	D116SLN_Co	D116NLC	D116NLC_Co
ZP (mV)		-24.1±0.0	-13.5±0.7	-18.3±0.2	-12.4±0.3
PCS (nm)		192.2±1.2	181.2±2.7	193.1±1.8	180.4±0.9
PI		0.224±0.027	0.175±0.027	0.245±0.035	0.181±0.045
LD (μm)	LD50	0.119±0.001	0.132±0.001	0.105±0.001	0.128±0.001
	LD90	0.259±0.002	0.320±0.001	0.199±0.005	0.296±0.004
	LD95	0.315±0.003	0.409±0.000	0.246±0.001	0.393±0.004
	LD99	0.466±0.007	0.573±0.002	0.364±0.082	0.579±0.003

The macroscopic appearance of the systems resembled a milky dispersion immediately after production and also after the cooling step.

The preparation of aqueous SLN and NLC dispersions with a mean particle size lower than 250 nm has been obtained in previous studies using only 5% of surfactant (Tyloxapol®) stabilizing 20% of lipid mass [118]. In this work, a relatively uniform size distribution has been obtained (PI < 0.250). Immediately after production, a unimodal with a relatively narrow size distribution was observed by LD measurements for all developed formulations. LD50% and LD90% were lower than 0.135 μm and 0.600 μm, respectively. The differences observed

between SLN and NLC, as well as the presence of drug molecules did not significantly change the particle size measured by PCS and LD.

Previous studies have shown that the non-ionic surfactant Tyloxapol® as a steric stabilizer of SLN could prevent gel formation and yield stable suspensions of nanoparticles based on Dynasan®116 [267]. Also for Dynasan®116-based SLN and NLC dispersions, the formation of semi-solid gels by Tyloxapol® stabilized SLN and NLC was not observed. Tyloxapol® molecules need to be organized in a specific steric arrangement at the droplet interface during the production step at high temperatures with the ethylene oxide chains protruding into the aqueous phase and stabilizing the system.

Due to the amphiphilic nature of Tyloxapol® dissolved in the aqueous phase prior to HPH with the melted lipid phase, it was expected that the corresponding SLN and NLC would be coated by its molecules. Therefore, the surfactant is able to change, i.e. extend the shear plane of the lipid particles, and consequently the ZP [320]. The incorporation of clotrimazole decreased the electrical charge at the surface of both SLN and NLC and, when comparing both systems, NLC also revealed lower ZP values than the respective SLN system. These results could be taken as an indication that clotrimazole is entrapped in the lipid matrix of SLN and NLC.

The pH values of all aqueous dispersions measurend immediately after production ranged between 5.5 and 6.0, showing no significant differences between the formulations.

4.1.1.2 At different temperatures of storage

The developed formulations have been stored at three different temperatures to challenge the systems under stress conditions. The assessment of physical stability at 4ºC, 25ºC and at 40ºC of storage has been performed one month after production of the aqueous dispersions. Table VI shows the obtained results.

In all storage temperatures, the systems remained in their colloidal particle size range (< 1 μm). The mean size was maintained lower than 250 nm, with a PI in the same magnitude as the values obtained immediately after production (PI < 0.250). LD50% and LD90% were lower than 0.200 μm and 0.650 μm, respectively. After one month of storage, all lipid nanoparticles showed a negative charge at their surface. Also the pH values did not vary notably between the variables investigated.

The differences between the evaluated parameters were not significant, neither under different storage temperatures nor with the presence of drug molecules, meaning that the systems are

physicochemically stable under stress conditions. No gel formation has been observed after one month of shelf life at three different temperatures. Tyloxapol® could stabilize the developed formulations even under stress conditions.

Table VI: Zeta potential and particle size parameters of Dynasan®116-based SLN and NLC formulations stored at different temperatures and obtained one month after production.

Sample	Storage temperature	ZP (mV)	PCS (nm)	PI	LD (µm)	
					LD50	LD90
D116SLN	4ºC	-21.6±0.1	227.4±0.9	0.205±0.004	0.188±0.013	0.590±0.051
	25ºC	-21.8±0.2	197.4±0.9	0.192±0.012	0.108±0.000	0.480±0.005
	40ºC	-22.1±0.7	174.1±1.1	0.191±0.018	0.097±0.001	0.295±0.001
D116SLN_Co	4ºC	-12.5±0.1	213.1±1.7	0.253±0.001	0.106±0.003	0.422±0.096
	25ºC	-12.3±0.1	201.5±3.2	0.233±0.019	0.159±0.006	0.555±0.007
	40ºC	-12.3±0.1	180.2±1.8	0.169±0.023	0.106±0.001	0.306±0.003
D116NLC	4ºC	-16.4±0.1	187.5±2.8	0.159±0.012	0.132±0.012	0.536±0.006
	25ºC	-16.4±0.1	173.9±1.1	0.248±0.009	0.107±0.000	0.500±0.001
	40ºC	-16.5±0.2	173.1±1.0	0.147±0.014	0.116±0.001	0.501±0.001
D116NLC_Co	4ºC	-11.1±0.1	189.5±0.2	0.186±0.033	0.198±0.006	0.647±0.006
	25ºC	-11.1±0.1	179.7±1.5	0.190±0.017	0.145±0.002	0.544±0.001
	40ºC	-11.1±0.1	177.1±1.0	0.165±0.013	0.158±0.003	0.602±0.003

4.1.1.3 During shelf life

From the literature, lipid nanoparticles dispersions with optimized stabilizer composition are physically stable on storage for several years [321]. For the present study, samples stored at room temperature have been evaluated concerning the physical parameters for two years. Table VII shows the obtained results.

During a period of two years no particle aggregation has been detected. The mean particle size remained lower than 200 nm for all developed formulations. The relatively small, homogeneously sized SLN and NLC displayed a satisfactory long-term stability (PI < 0.250). LD50% and LD90% were lower than 0.300 µm and 0.700 µm, respectively. After two years of storage at room temperature all nanoparticles revealed a negative charge at their surface.

The lowest ZP values were obtained for D116NLC_Co, being -8.4 mV. Although this value is extremely low for electrostatic stabilization of nanoparticles (an optimized formulation should have ZP values between -30 mV and -60 mV [293]), these latter showed good physical stability.

The stability has also been monitored by macroscopic observations. All developed systems remained with a milky-like appearance without particle sedimentation or creaming during the same period of time. Once the used model drug clotrimazole has lipophilic properties (water solubility lower than 0.01 mg/ml at 25ºC [273]), it is clearly possible that it remains entrapped into the lipid matrix. In fact, precipitation of drug has not been observed. Dynasan®116-based lipid nanoparticles could be stabilized with a single non-ionic surfactant. Such systems did not display any tendency to form gels, neither macroscopic particles nor aggregates formed upon storage.

Table VII: Zeta potential and particle size parameters of Dynasan®116-based SLN and NLC formulations obtained after one day (D1), one year (Y1) and two years (Y2) of storage at 25ºC.

Sample	Storage time	ZP (mV)	PCS (nm)	PI	LD (µm)	
					LD50	LD90
D116SLN	D1	-23.1±1.0	203.6±1.8	0.219±0.003	0.107±0.000	0.492±0.001
	Y1	-20.1±0.1	184.9±2.9	0.217±0.014	0.108±0.001	0.463±0.015
	Y2	-11.4±0.5	171.7±3.4	0.154±0.048	0.102±0.001	0.310±0.008
D116SLN_Co	D1	-12.3±0.9	201.4±4.7	0.220±0.021	0.273±0.007	0.803±0.012
	Y1	-11.0±0.1	198.4±2.6	0.196±0.045	0.150±0.007	0.607±0.035
	Y2	-10.8±0.6	149.7±4.2	0.213±0.056	0.097±0.000	0.283±0.003
D116NLC	D1	-16.7±1.0	181.2±2.7	0.175±0.027	0.132±0.001	0.573±0.002
	Y1	-16.2±0.1	171.3±1.9	0.180±0.032	0.106±0.000	0.477±0.013
	Y2	-14.3±0.1	176.8±4.6	0.148±0.077	0.238±0.002	0.642±0.004
D116NLC_Co	D1	-10.5±1.1	182.3±1.9	0.182±0.021	0.189±0.003	0.645±0.002
	Y1	-9.6±0.2	177.6±4.2	0.220±0.017	0.163±0.007	0.634±0.013
	Y2	-8.4±0.1	188.1±9.6	0.215±0.120	0.214±0.003	0.574±0.006

4.1.2 Imaging analysis of Dynasan®116-based lipid nanoparticles

By light microscopy analysis the absence of aggregation phenomena of Dynasan®116-based SLN and NLC has also been confirmed immediately after production, and also by monitoring the particle growth during storage time at room temperature.

SEM analysis has been performed to evaluate the potential differences in particle shape and morphology of SLN formulations. Once aqueous NLC dispersions are composed of a liquid lipid component (Miglyol®812) inside their matrix, the preparation of the sample previously to SEM analysis resulted in particle disruption and therefore SEM pictures of those particles could not be obtained. Fig. 4.2 compares the results obtained one week and one year after production of aqueous SLN dispersions.

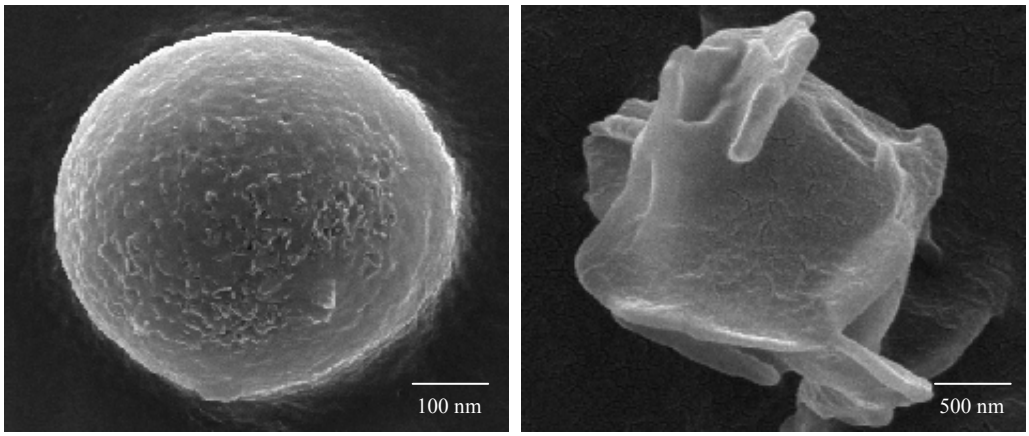

(a) SEM of SLN one week after production (b) SEM of SLN one year after production

Fig. 4.2: SEM pictures of Dynasan®116-based lipid nanoparticles. (a) SLN with 600 nm, obtained one week after production; (b) SLN with 500-1000 nm, obtained one year after production.

Spherical Tyloxapol®-stabilized SLN with a particle size of 600 nm (Fig. 4.2, a) were observed after one week of storage at room temperature. This reveals that lipid is rearranged in a more unstable α polymorphic form, which is less anisometric than those of stable β polymorphic forms, indicating that major rearrangements may take place in SLN during storage time [303]. After one year of storage those particles reveal a platelet-like shape (Fig. 4.2, b) having a layered structure, which is characteristic of tripalmitin nanoparticles [322]. The aging of SLN caused polymorphic modifications in the lipid matrix revealing a more platelet structure after one year of storage at room temperature. Usually the platelet-like structures exhibit a thickness of less than 50 nm. The analysis of SLN of one year old shows particle aggregation during SEM procedure due to the lipid nature of these systems (Fig. 4.2, b).

4.1.3 Assessment of the physicochemical stability of clotrimazole

The production of Dynasan®116-based lipid nanoparticles is performed at high temperatures (approximately 80ºC), a condition that might destroy sensitive compounds. In order to evaluate the chemical stability of clotrimazole at high temperatures, a complementary thermal analysis of this drug has been performed by TGA. Fig. 4.3 shows the TGA pattern of pure clotrimazole, representing the weight loss of the sample as a function of temperature.

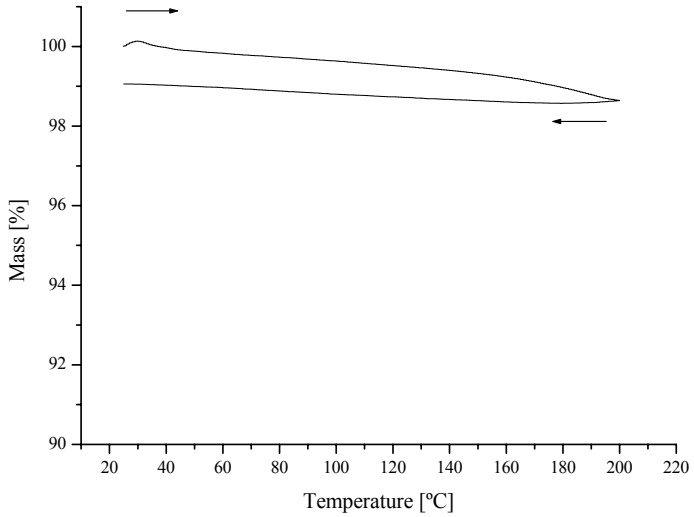

Fig. 4.3: TGA pattern of pure clotrimazole.

Once the melting point of this drug has been recorded at approximately 145ºC (Fig. 4.4) this analysis has been performed heating the sample from 25ºC to 200ºC and cooling it again from 200ºC to 25ºC. No mass depending decomposition was detected in the temperature range of 25ºC to 200ºC, at a heating rate of 10 K/min. At temperatures above the recorded melting point of clotrimazole the pure drug melted showing no mass variation during the heating and cooling runs. This result emphasizes the fact that the drug is chemically stable under the production conditions applied for the preparation of drug-loaded SLN and NLC by HPH, which means that at least it does not suffer decomposition under weight loss.

The dispersions were prepared above the melting point of the solid lipid (Dynasan®116), at approximately 80ºC [303] (the recorded melting point for tripalmitin was 64ºC [133]). For the production of clotrimazole-loaded lipid nanoparticles the drug has been dissolved in the melted lipid or lipid mixture until an optically clear liquid was obtained at 80ºC. Thus, clotrimazole needs to be chemically stable at this temperature, so TGA and DSC were recorded for pure drug.

In order to determine the melting point of clotrimazole and the enthalpy of the melting event, the drug was analysed before and after tempering it by incubation for 1 hr in an oven heated at 90ºC, which is five times higher than the heat exposure during the production of lipid nanoparticles by HPH. Fig. 4.4 shows the obtained patterns.

A melting range between 141º and 145ºC for clotrimazole has been previously reported [273]. Both DSC curves of this drug depicted a single sharp endotherm with an extrapolated onset temperature of 143ºC. Clotrimazole melted at 144.75ºC before tempering showing an enthalpy of 94.24 J/g (Fig. 4.4, upper). The melting point value slightly increased to 145.14ºC, while the enthalpy decreased to 93.36 J/g (Fig. 4.4, lower) when the drug was heated for 1 hr at 90ºC.

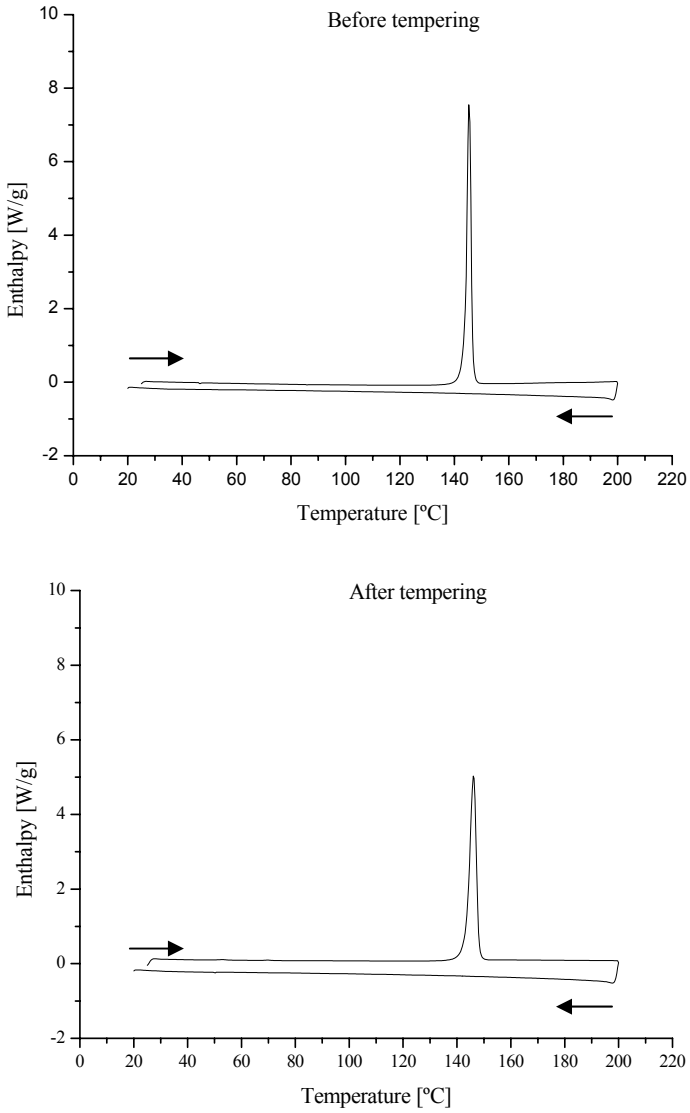

Fig. 4.4: DSC patterns of pure clotrimazole before (upper) and after (lower) tempering the drug under heat exposure (90ºC) for 1 hr.

X-ray diffraction will definitely confirm the different molecular organization within the solid while thermal analytical methods provide useful additional information. Fig. 4.5 shows the WAXS analysis of clotrimazole before and after tempering at 90ºC for 1 hr. In the following WAXS curves the plots have been displaced vertically for better visualization. The units of intensity are arbitrary.

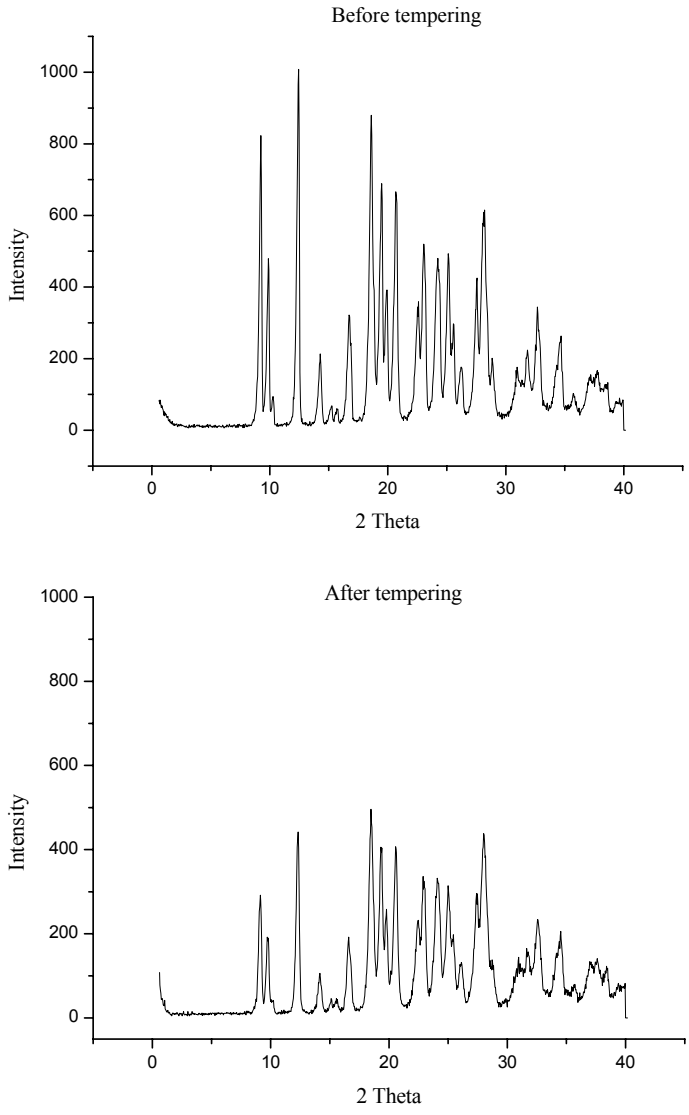

Fig. 4.5: X-ray diffraction patterns of pure clotrimazole recorded before (upper) and after (lower) tempering the drug under heat exposure (90ºC) for 1 hr.

Because of the different internal organization within the solid, polymorphs may show different melting points, solubilities, chemical reactivity or stability. These can have an impact on pharmaceutical properties such as dissolution rate and bioavailability.

Unfortunately, polymorphism is common among pharmaceutical substances and the evaluation of new drug entities for polymorphism is important in early pre-formulation studies. Varying the polymorphic form for a particular drug substance can change its chemical and physical stability due to the changes in reactivity and in the rate of dissolution of the solid substance. As the rate of dissolution can be related to the degree of absorption, particularly of less soluble compounds, polymorphism may have an effect on the therapeutic activity of those forms whose polymorphic nature was not controlled.

Clotrimazole showed a crystalline state (Fig. 4.5, upper), revealing less peaks intensity after heat exposure (Fig. 4.5, lower). Clotrimazole has the same profile however with lower intensity after heat exposure revealing no polymorphism.

4.1.4 Assessment of the polymorphic behaviour of lipid and drug

As exposed before, aqueous dispersions of lipid nanoparticles are not composed exclusively of lipid compounds. They include drug and surfactant molecules, which might change the polymorphic behaviour of lipid when dispersed in a water phase. The aim of the present study was the assessment of polymorphic behaviour of lipid during the production process of Dynasan®116-based SLN and NLC, as well as the assessment of its structure in form of lipid nanoparticles.

4.1.4.1 Characterization of the bulk Dynasan®116

In general, the method of preparation of SLN and NLC changes the polymorphism of the lipid, which is frequently different in the formulation after solidification, in comparison to the bulk material [2]. Therefore, the bulk Dynasan®116 has been analysed by DSC (Fig. 4.6) before and after tempering for 1 hr at 90ºC. Table VIII shows the corresponding DSC data.

The first heating curve (Fig. 4.6, upper) revealed an onset temperature of approximately 61ºC, corresponding to the β' modification of Dynasan®116. The β form of the lipid melted at 64.21ºC. Note that lipid nanoparticles were prepared by hot HPH. This means that the lipid was melted at 80ºC followed by the drug dissolution process, in case of production of drug-loaded nanoparticles. A pre-emulsion was obtained after dispersing the melted lipid phase in the hot Tyloxapol® solution. The pre-emulsion was passed through the high pressure homogenizer to obtain a hot o/w nanoemulsion, which has been cooled, recrystallizing the lipid and forming the SLN or NLC.

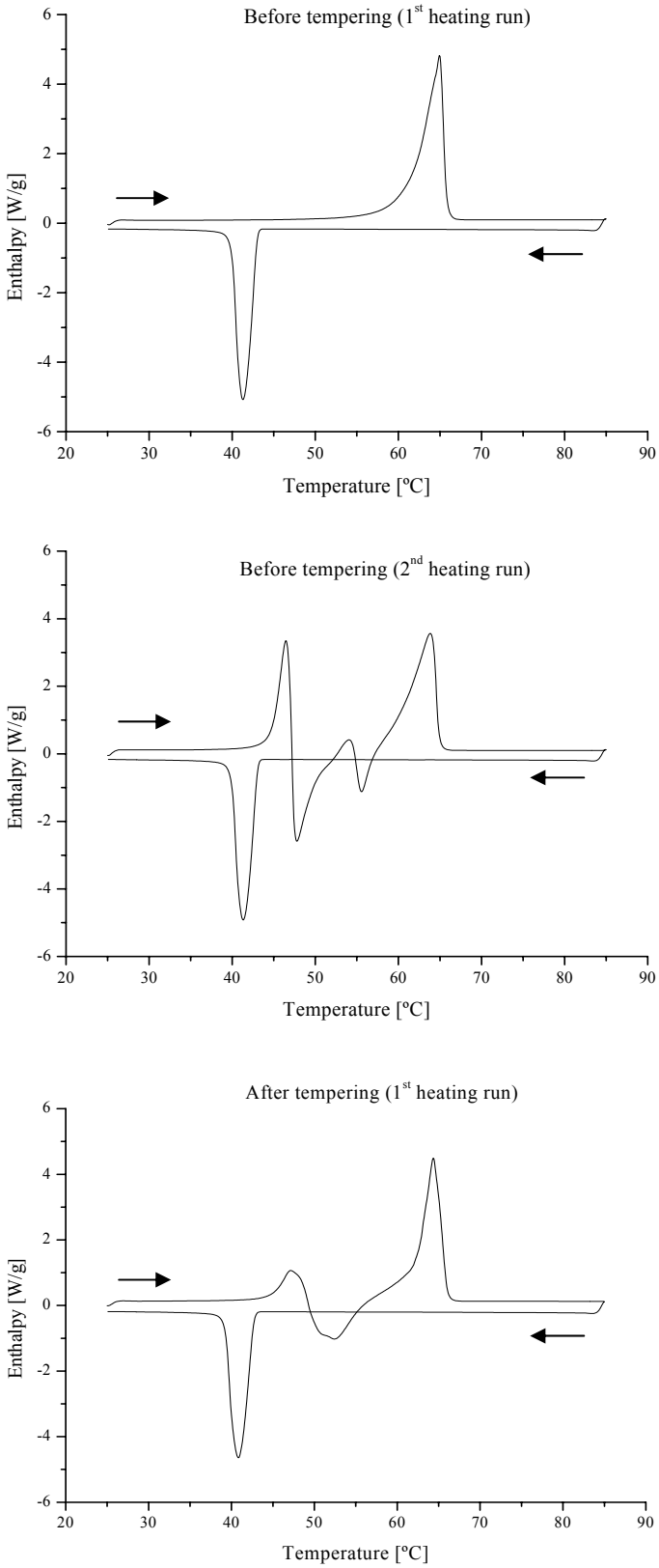

Fig. 4.6: DSC patterns of bulk Dynasan®116 recorded before (upper and middle) and after (lower) tempering the lipid under heat exposure (90ºC) for 1 hr.

When analysing aqueous SLN or NLC dispersions by DSC, the lipid has been melted before, meaning that it is a second heating run (Fig. 4.6, middle). The recorded onset temperature in this curve was 44.63ºC, which corresponds to the α modification. With regard to the melting enthalpy values the decrease was from 182.60 J/g to 115.49 J/g, showing a significant difference between those curves (upper and middle, Fig. 4.6). Concerning the first heating run after tempering (Fig. 4.6, lower), it is visible the less pronounced polymorphic forms (smaller maxima and shoulders) of Dynasan®116 in comparison to curve that corresponds to the second heating run (middle).

The first peak of the last two heating curves (Fig. 4.6, middle and lower) recorded at approximately 44.6ºC corresponds to the fraction of the unstable α form, which is more pronounced in the second heating run before tempering than in the first heating run after tempering. The cooling curves of the three runs are identical.

Table VIII: DSC parameters of bulk Dynasan®116 recorded before and after tempering the lipid under heat exposure (90ºC) for 1 hr.

Curves of bulk Dynasan®116	Melting point (ºC)	Onset (ºC)	Integral (mJ)	Enthalpy (J/g)
First heating run before tempering	64.21	60.98	826.27	182.60
Second heating run before tempering	63.32	44.63	522.58	115.49
First heating run after tempering	61.76	44.63	784.00	119.09

The DSC data show that the melting points differ by 1ºC to 2ºC, whereas the onset temperatures differ by 11ºC. The second sample shows an additional shallow endotherm at a temperature below that of the main transition, therefore, after tempering the lipid is now a mixture of isomers.

In the case of DSC, the heating rate might be very important in the detection of the presence of polymorphism. Additional peaks were discernible at lower heating rates. This is due to less stable forms melting and recrystallizing previously to the more stable melting form β. The result is a melting endotherm, a recrystallization exotherm and a final melting endotherm. It is particularly important to distinguish between endotherms due to melting of a less stable polymorphic form prior to recrystallization and a second endotherm due to melting of a more stable form, and endotherms attributed to desolvation followed by melting of the desolvate form. The endoterms are due to solid-solid transitions as the less stable polymorphs convert to the more stable form. Conditioning samples of the lower stable polymorphs at temperatures below their melting points showed the loss of DSC endotherms for the less stable polymorph.

Typical DSC traces for the newly crystallized lower stable polymorph show the solid-solid transitions at low scanning rates (2.5-10 K/min) but at higher temperature scanning rates only the melting endotherms of the two polymorphs could be discerned. The high scanning rate traces show exotherms due to recrystallization of the more stable melting polymorph from melts of the less stable polymorph.

WAXS analysis has also been used to investigate the lamellae arrangement of the lipid molecules and the crystallinity of the fatty acid chains in the acylglycerols of Dynasan®116. WAXS analysis of Dynasan®116 was performed without pre-treatment (Fig. 4.7, upper) and after tempering the lipid at 90ºC for 1 hr (Fig. 4.7, lower).

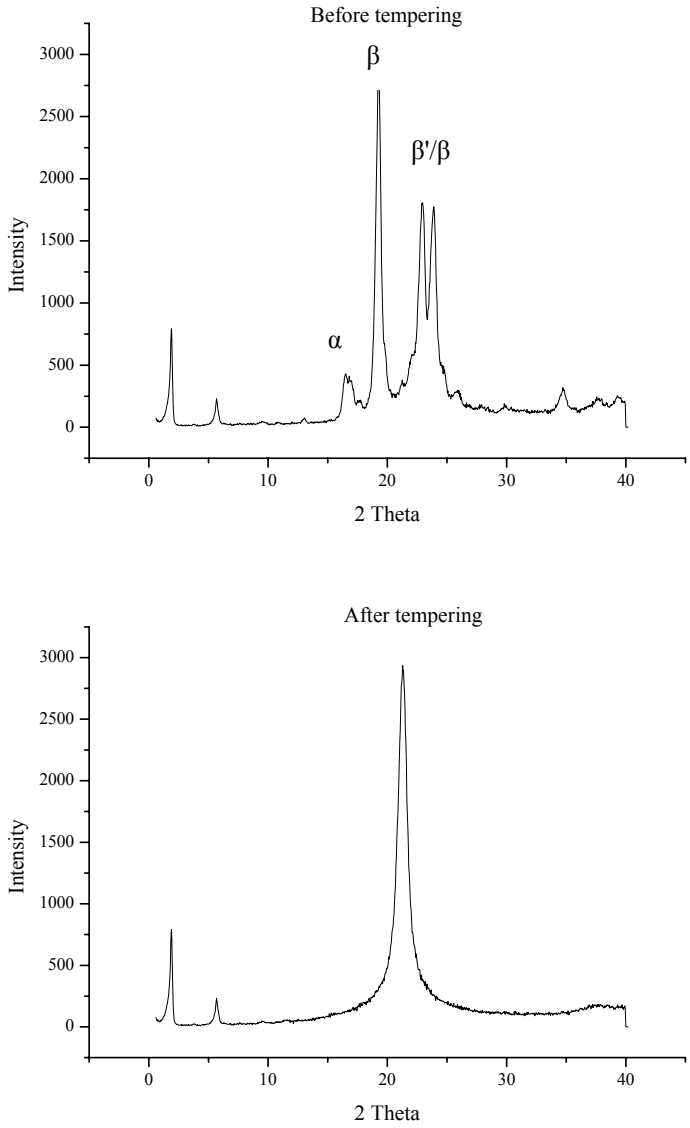

Fig. 4.7: X-ray diffraction patterns of bulk Dynasan®116 recorded before (upper) and after (lower) tempering the lipid under heat exposure (90ºC) for 1 hr.

The applied thermal treatment imitates the heating of the lipid for dissolution of clotrimazole during the lipid nanoparticles preparation. In Fig. 4.7 it is clearly visible the differences of the lamellae arrangements of the fatty acid chains of the triacylglycerols. Before the melting step, the lipid shows the three typical signals of triacylglycerols (α, β' and β) [323, 324]. However, in the X-ray diffractogram of the melted lipid after tempering a different organization of the lipid lattice was observed. Only one peak at 21.36 (2θ) with an interplanar distance of 0.423 nm, having a shoulder at 23.36 (2θ, d = 0.389 nm), was recorded. This means that the mixture is in a less crystalline state.

4.1.4.2 Characterization of the physical mixtures of bulk lipid and drug

The polymorphic modifications of Dynasan®116 and clotrimazole have been investigated by DSC and by X-ray diffraction, because they are important parameters that affect the drug incorporation in the particle matrix. Once clotrimazole has a crystalline character a melting event should be detected in the DSC runs of physical mixtures of drug and lipid.

4.1.4.2.1 DSC analysis

DSC analysis of the physical mixtures of 1% (m/m) drug and bulk Dynasan®116 revealed only the melting events of the lipid at 64.70ºC (enthalpy of 182.67 J/g) showing that the drug is obviously dissolved in the lipid (Fig. 4.8, upper). This means that clotrimazole is molecularly dispersed in the lipid phase. After tempering the mixture, the melting point slightly decreased to 61.45ºC, revealing an enthalpy of 176.08 J/g (Fig. 4.8, lower). Table IX shows the registered DSC parameters.

The observed results do not support a crystalline character of clotrimazole, on the contrary, reveal that the drug is dissolved in the melted lipid. Based on the production process, the physical mixtures were heated from 25ºC to 85ºC to give clotrimazole the possibility to dissolve to its maximum solubility, then the mixtures were cooled in order to recrystallize (Fig. 4.8, upper). This procedure imitates the production process of the lipid nanoparticles. Then the mixtures were heated a second time (Fig. 4.8, lower).

The second heating curve corresponds now to the heating of the produced aqueous SLN or NLC dispersions, meaning that a fraction of the lipid matrix of the prepared nanoparticles might also be in an amorphous state. After running a second heating of the physical mixture, the presence of the polymorphic α form was detected at approximately 46ºC (Fig. 4.8, lower).

Concerning the cooling curves only minor differences were detected between both curves (Fig. 4.8). Once the NLC system is also composed of an oil fraction, the physical mixtures of solid lipid, liquid lipid and drug have been analysed by DSC as well (Fig. 4.9).

Distortion of the crystal lattice of Dynasan®116 increased with the presence of Miglyol®812 in the mixture leading to a reduction of the onset temperature and melting peak (Fig. 4.9, Table X).

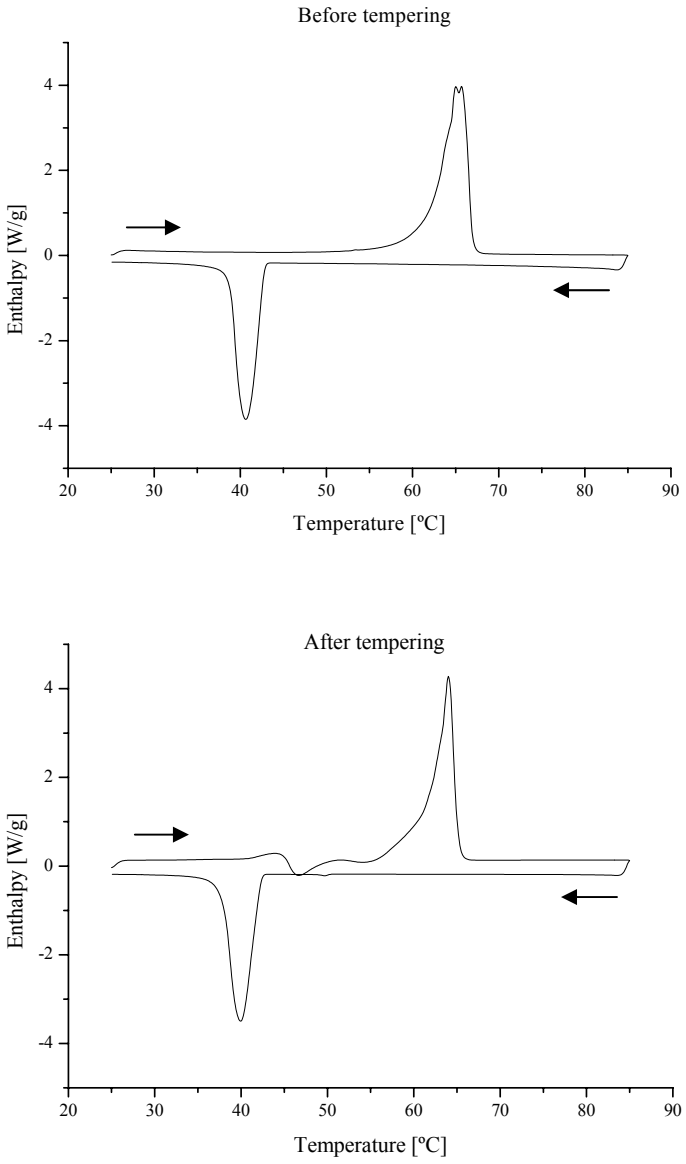

Fig. 4.8: DSC patterns of physical mixtures of Dynasan®116 and clotrimazole (99+1) recorded before (upper) and after (lower) tempering the mixture under heat exposure (90ºC) for 1 hr.

Table IX: DSC parameters of physical mixtures of Dynasan®116 and clotrimazole (99+1) recorded before and after tempering the mixture under heat exposure (90ºC) for 1 hr.

Curves of physical mixtures of Dynasan®116 and clotrimazole	Melting point (ºC)	Onset (ºC)	Integral (mJ)	Enthalpy (J/g)
Before tempering	64.70	62.32	1415.00	182.67
After tempering	62.87	61.45	1450.93	176.08

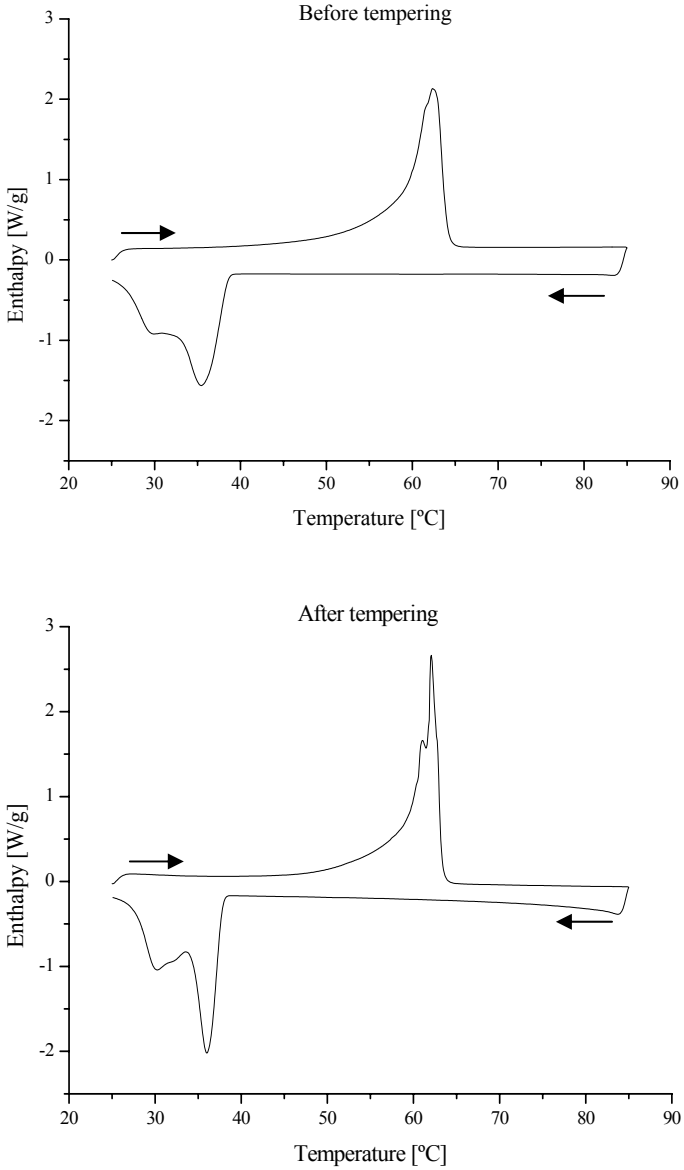

Fig. 4.9: DSC patterns of physical mixtures of Dynasan®116, Miglyol®812 and clotrimazole (69.3+29.7+1) recorded before (upper) and after (lower) tempering the mixture under heat exposure (90ºC) for 1 hr.

Before tempering the mixture of Dynasan®116, Miglyol®812 and clotrimazole, the presence of the stable polymorph β of the lipid was hardly detected, while after tempering the presence of β form was recorded at approximately 64ºC. Before tempering, the heating curve revealed a less pronounced shoulder, which corresponds to the β' modification of tripalmitin. After tempering no more shoulder was visible being substituted by a well defined small peak at approximately 62ºC. The main peak in both curves corresponds to the stable β modification. The influence of Miglyol®812 was also observed during the cooling process in both curves. Concerning the cooling curves, the peak recorded between 40ºC and 25ºC both before and after tempering shows the presence of Miglyol®812. The difference of shape between them is due to the presence of well defined polymorphic modifications.

Table X: DSC parameters of physical mixtures of Dynasan®116, Miglyol®812 and clotrimazole (69.3+29.7+1) recorded before and after tempering the mixture under heat exposure (90ºC) for 1 hr.

Curves of mixtures of Dynasan®116, Miglyol®812 and clotrimazole	Melting point (ºC)	Onset (ºC)	Integral (mJ)	Enthalpy (J/g)
Before tempering	61.31	58.49	1871.83	123.60
After tempering	61.48	60.52	784.60	109.29

The calculated melting enthalpy of the lipid fraction in the mixtures shows little difference in comparison to the melting enthalpy of the bulk Dynasan®116. Based on this observation, it can be stated that all mixtures might be preferentially in the β' modification with an onset temperature higher than 40ºC. This is the main pre-requisite for preparation of lipid nanoparticles for topical drug delivery. Taking into account that the lipid particle matrix should be in the solid state at skin temperature (32ºC), the selected mixtures seem to be appropriated for the preparation of clotrimazole-loaded SLN and NLC. The endotherms recorded in Fig. 4.9 show the crystals of Miglyol®812 (small shoulder) of the main peak of the cooling scan.

4.1.4.2.2 X-ray diffraction analysis

Concerning WAXS studies, Fig. 4.10 shows the physical mixtures of Dynasan®116 and clotrimazole (99+1) recorded before and after tempering the mixture under heat exposure (90ºC) for 1 hr. Again, the obtained results confirm the ones reported from the DSC curves.

Before tempering the mixture does not show drug-lipid interaction, and the curve depicts the typical polymorphic forms of tripalmitin. After tempering only one peak has been recorded showing the β form of the lipid.

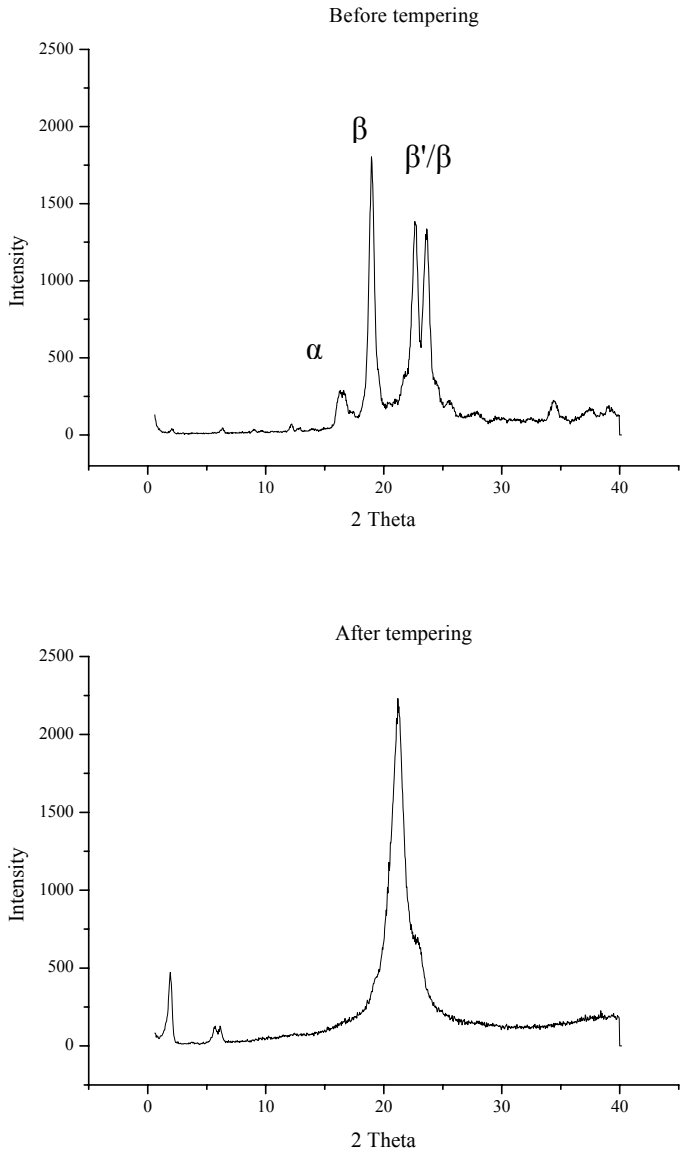

Fig. 4.10: X-ray diffraction patterns of physical mixtures of Dynasan®116 and clotrimazole (99+1) recorded before (upper) and after (lower) tempering the mixture under heat exposure (90ºC) for 1 hr.

The same procedure has been performed for physical mixtures of clotrimazole, Dynasan®116 and Miglyol®812 and the results are shown in Fig. 4.11. Interestingly, the same patterns were observed, however with different intensity, before (Fig. 4.11, upper) and after (Fig. 4.11, lower) tempering the mixtures at 90ºC for 1 hr.

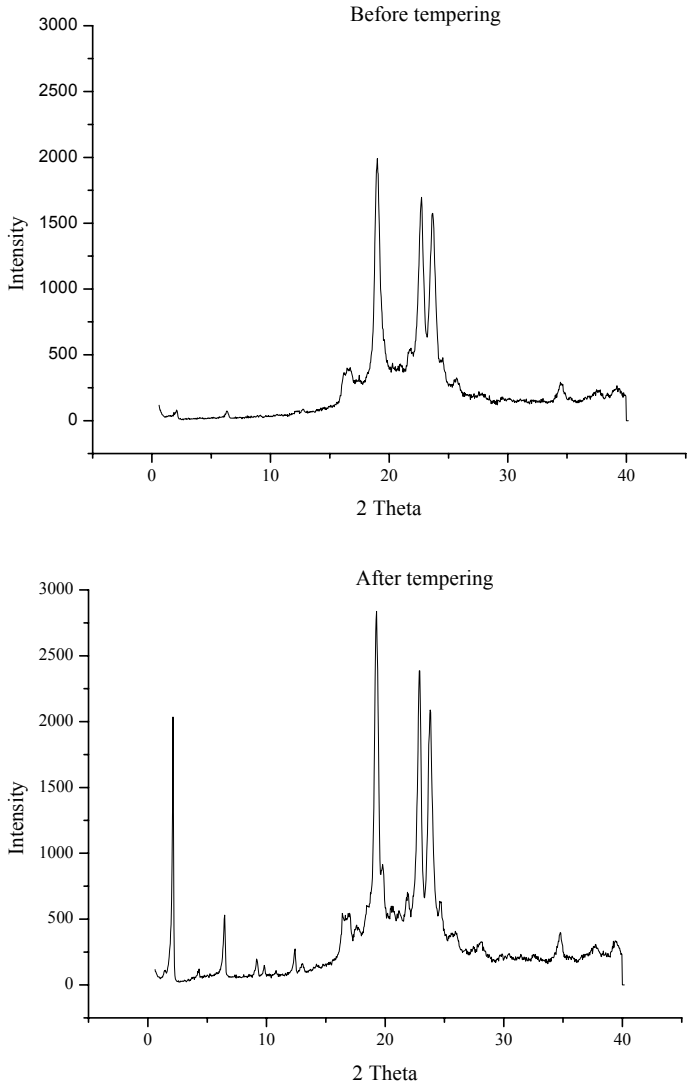

Fig. 4.11: X-ray diffraction patterns of physical mixtures of Dynasan®116, Miglyol®812 and clotrimazole (69.3+29.7+1) recorded before (upper) and after (lower) tempering the mixture under heat exposure (90ºC) for 1 hr.

Tempering the mixture of the three components maintained the crystallinity of the side chains proven by the detection of the same patterns. It can, therefore, be concluded that the obtained X-ray data are in agreement with the reported DSC results. This means that the NLC recrystallize directly in the long-term stable crystal lattice.

4.1.4.3 Characterization of the Dynasan®116-based SLN and NLC

Admixture of different types of surfactants with bulk triacylglycerols can have pronounced effects on the kinetics of polymorphic transitions of the lipid material after its crystallization [323]. The influence of the surfactant composition on the polymorphism of triacylglycerols has also been observed for colloidal triacylglycerol dispersions [325]. In dispersions, the type of surfactant may influence the crystallization temperature of the dispersed phase as observed for dispersions of emulsified lipid systems. Crystallization temperature and polymorphic transitions are important parameters for the preparation of triacylglycerol nanoparticles. During preparation, the emulsified dispersion must be cooled below the critical crystallization temperature of the triacylglycerols (i.e. much below their melting temperature) to crystallize the nanoparticles. If this critical temperature is not reached, the particles remain in the liquid state and an emulsion of supercooled, liquid particles is obtained rather than the desired triacylglycerol dispersion [133]. Transition into a more stable triacylglycerol polymorph is usually related to a rearrangement of the triacylglycerol molecules with increasing the lattice density [254, 326]. The type of crystal polymorph obtained and the kinetics of the transitions may thus have important consequences for the stability of the dispersion, as well as for the drug loading. Studies about the influence of surfactants on the crystallization process may provide deeper insight into the type of interaction of the dispersed lipid with the surfactant used for the steric stabilization.

Polymorphic transformations may occur during the preparation of lipid drug delivery systems and during the subsequent storage time [3, 33, 327]. After the HPH step and during cooling of the nanoemulsion the melted lipid solidifies and the triacylglycerol molecules can crystallize in different polymorphic forms, depending on the composition of the lipid and the cooling rate. Regarding the lipid composition, nanoparticles made from mixed triacylglycerols are characterized by more imperfections in the crystal lattice, while the ones made from monoacid triacylglycerols have a higher degree of crystalline order and may be related to lower drug loading capacities [33, 96]. Concerning the cooling rate, it is known that due to a fast solidification during the preparation of lipid nanoparticles the unstable α modification is preferentially formed. During a slow solidification process, the lipid molecules can arrange in the thermodynamically most stable β modification [323].

According to the X-ray investigations, the complex melting behaviour of triacylglycerols is due to a stepwise melting of the β stable form [303]. For the β modification of such molecules, several sub-modifications, which differ in the angle of chain tilt and thus in their

long spacings, have been described. Thermodynamic stability and lipid packing density increase, while drug incorporation rates decrease in the following order: supercooled melt, α modification, β' modification and β modification [12].

Supercooled melts are not lipid suspensions, rather systems similar to o/w emulsions [223]. They describe a phenomenon that lipid crystallization may not occur although the sample is stored at a temperature below the melting point of the lipid. These systems are not unusual in lipid nanoparticles preparation [328]. The main reason for the formation of supercooled melts is the size dependence of crystallization processes. In order to start, crystallization requires a critical number of crystallization nuclei [329]. This critical number of molecules is less likely to be formed in small droplets and therefore, the tendency for the formation of supercooled melts increases with decreasing of the droplet size. The range of supercooling (difference of temperatures between the melting and crystallization points) can reach 30ºC to 40ºC in lipid dispersions [330]. In addition to size, crystallization can be affected by surfactants, incorporated drugs and other factors. Since immobilization of drug molecules in nanoparticles of supercooled melts is not expected to occur in the same way as in solid nanoparticles (SLN and NLC), it is necessary to evaluate the solid state of the lipid by DSC and X-ray diffraction. Therefore, lipid nanoparticles without drug and clotrimazole-loaded were also characterized by DSC and by WAXS analysis.

4.1.4.3.1 DSC analysis

Tables XI and XII show the obtained DSC results, of Dynasan®116-based SLN and NLC dispersions, respectively, after seven days (D7) and one (Y1) and two (Y2) years of storage at three different temperatures.

In all developed formulations the value of the melting temperature increased with the shelf life at different storage conditions. In comparison to the DSC results obtained for the bulk Dynasan®116 (Fig. 4.6, Table VIII) the aqueous SLN and NLC dispersions (drug-free and drug-loaded) showed lower onset temperature and peak temperature values, as well as the calculated melting enthalpies in all storage temperatures and during a shelf life of two years. These results indicate that the lipid partially changed from the β' modification (in the bulk) to the α modification in the lipid nanoparticles.

At room temperature (25ºC), the melting events of SLN and NLC showed similar values ranging from 58ºC to 60ºC for SLN, with onset temperatures between 54ºC and 56ºC, and from 56ºC to 60ºC for NLC, with onset temperatures between 51ºC and 56ºC. It is also

important to emphasize the fact that after two years all formulations could be melted at temperatures lower than 63ºC (melting point of bulk Dynasan®116), however at values higher than 40ºC (pre-requisite for topical administration of lipid nanoparticles).

Table XI: DSC parameters of aqueous Dynasan®116-based SLN dispersions recorded after seven days (D7) and one (Y1) and two (Y2) years of storage at three different temperatures.

DSC parameters		D116SLN			D116SLN_Co		
		4ºC	25ºC	40ºC	4ºC	25ºC	40ºC
mp (ºC)	D7	59.01	59.46	59.64	58.72	59.07	58.88
	Y1	60.82	61.42	61.63	60.79	60.63	61.50
	Y2	60.70	60.38	61.46	60.27	60.24	61.19
Onset (ºC)	D7	55.23	55.53	55.61	56.53	54.97	54.40
	Y1	57.14	57.25	58.54	56.66	56.49	58.15
	Y2	57.05	57.21	58.59	56.69	56.92	57.96
Integral (mJ)	D7	172.41	295.72	870.01	392.63	358.95	532.34
	Y1	824.14	977.88	1001.20	1056.51	791.49	1019.42
	Y2	845.76	363.23	700.55	700.34	358.72	846.49
Enthalpy (J/g)	D7	34.12	33.67	34.23	30.58	30.85	30.42
	Y1	37.16	36.44	37.32	34.52	34.63	36.50
	Y2	37.26	38.62	39.56	35.65	35.49	38.18
RI (%)	D7	89.02	87.03	83.29	82.43	79.74	79.74
	Y1	91.61	89.70	85.28	86.41	83.31	83.31
	Y2	93.81	91.61	90.27	96.49	91.74	91.74

Concerning the RI, which is a measure of the amount of solid content inside SLN and NLC, it is perfectly visible the higher solid character of SLN formulations in comparison to NLC formulations. Note that both systems are prepared with the same lipid concentration, however for the preparation of NLC 30% of Dynasan®116 has been replaced by Miglyol®812, which is a liquid of medium chain triacylglycerols (C_8-C_{10}), having a density between 0.945 and 0.955 g/cm^3, with a recrystallization temperature at -29.6ºC determined by DSC at a cooling rate of 5 K/min [164]. With storage time all samples also showed increased values of RI, as expected.

The dispersed tripalmitin crystallizes, as expected much below its melting temperature and the crystallization temperature of the bulk material [133]. Although the effect of the stabilizer

in the crystallization of these systems has not been investigated, it is known that a crystallization enhancing effect has been described in the case of dispersed lipid material for stabilizers with a chain structure similar to that of the dispersed substance [331].

Table XII: DSC parameters of aqueous Dynasan®116-based NLC dispersions recorded after seven days (D7) and one (Y1) and two (Y2) years of storage at three different temperatures.

DSC parameters		D116NLC			D116NLC_Co		
		4ºC	25ºC	40ºC	4ºC	25ºC	40ºC
mp (ºC)	D7	56.49	58.04	60.42	56.51	58.12	60.31
	Y1	56.95	61.00	61.83	57.92	60.70	61.47
	Y2	57.51	61.41	61.94	58.24	60.91	61.98
Onset (ºC)	D7	51.44	54.22	54.60	51.01	54.57	55.21
	Y1	52.42	58.61	59.99	53.61	58.32	59.82
	Y2	52.74	58.57	60.07	53.79	58.40	60.14
Integral (mJ)	D7	490.35	164.33	6.6	688.90	156.02	12.24
	Y1	706.51	32.22	19.62	699.87	86.14	17.81
	Y2	465.48	12.64	20.36	596.73	43.81	15.88
Enthalpy (J/g)	D7	24.87	17.88	0.39	23.02	15.79	0.68
	Y1	28.33	1.28	0.86	27.00	4.49	0.84
	Y2	27.32	1.31	0.90	26.01	3.07	0.64
RI (%)	D7	44.95	43.27	39.68	45.21	40.82	38.28
	Y1	49.17	48.96	44.82	47.77	46.48	41.80
	Y2	50.82	48.75	44.87	48.57	43.56	40.63

A templating mechanism, where the stabilizer chains act as the ordering principle leading to nucleation at higher temperatures, is often discussed as the cause for crystallization. Even thought that Tyloxapol® has a hydrophobic portion with high affinity to the fatty acid chains of the dispersed triacylglycerols, it does not act as a crystallization enhancing template at the interface. In the case of o/w emulsions containing hydrophobic emulsifier additives with long, saturated fatty acid chains in the oil droplets, the increased crystallization tendency of the dispersed phase has been correlated with the formation of crystalline hydrophobic emulsifier templates in the oil droplets. Previous investigations on tripalmitin nanoparticles also indicated that rigid surfactant chains are needed to induce crystallization of tripalmitin at

higher temperatures [331]. The hydrophobic chains of the Tyloxapol® molecules are probably too mobile to induce crystallization at elevated temperatures.

The melting behaviour of triacylglycerol nanoparticles strongly depends on the particle size, irrespective of the matrix material and of the stabilizer composition. From thermodynamics, it is expected that the melting temperature of colloidal substances would decrease with particle size. Models based on the Thompson equation modified for crystalline materials, or the well known Gibbs-Thompson equation, are often used to describe the particle size dependence of the melting temperature. They are described using the equation 25:

$$-\frac{T_0 - T}{T_0} \approx \ln\frac{T}{T_0} = -\frac{2\gamma_{sl} V_s}{r \Delta H_{fus}} \qquad (25)$$

where T is the melting temperature of a particle with radius r, T_0 is the melting temperature of the bulk material at the same external pressure, γ_{sl} is the interfacial tension at the solid-liquid interface, V_s is the specific volume of the solid, and ΔH_{fus} is the specific heat of fusion. It has been shown that this equation does not apply for spherical (curved) particles but can be used to describe the behaviour of particles with plane surfaces. Therefore, the Gibbs-Thompson equation can be used to explain the melting point depression of triacylglycerols nanoparticles compared to their bulk lipid phase. For the size dependence of the melting point of inorganic particles, in particular, modified models are frequently used to account for deviations from the predicted linear relationships between relative melting point depression and particle curvature (1/r) frequently observed with such particles [2]. A shift of the melting transition to lower temperatures with decreasing mean particle size was also observed for the Dynasan®116 dispersions under investigation (Tables XI and XII), meaning that the smaller particles melt at lower temperatures. The course of the melting process of small size triacylglycerol particles is very unusual once all finely dispersed matrix materials exhibited a more or less stepwise melting event. The structure of very fine particles thus differs significantly from that in the bulk or in coarser colloidal particles. The existence of only one additional, low melting structure in very fine particles is, however, not sufficient to explain the complex melting behaviour of the dispersions at higher temperatures.

Because of the length of the triacylglycerol chains, the differences in possible platelet heights are of colloidal size, and at least for thin particles, cannot be neglected in relation to the overall platelet height. By assuming that the relation γ_{sl}/r in the Gibbs-Thompson equation for crystals is more precisely expressed by γ_x/r_x where the relative dimensions of a crystal in equilibrium are interrelated via the interfacial tensions γ_x of the corresponding crystal faces by:

$$\frac{\gamma_x}{r_x} = \frac{\gamma_1}{r_1} = \frac{\gamma_2}{r_2} = \frac{\gamma_3}{r_3} = \text{constant} \quad (26)$$

Half of the height of a nanocrystal may be used as the size parameter in the Gibbs-Thompson equation (where γ_x is the interfacial tension of the surface x and r_x is the distance between the crystal surface x and the centre of the crystal. Since the height of the triacylglycerol nanoparticles can only change in steps corresponding to the thickness of the single triacylglycerol layers reflected by the d_{001} value, this will result in distinct melting temperatures reflecting the differences in particle height. Each of the individual transitions observed in the melting event would thus be due to the melting of a class of particles with a well defined platelet height.

By adding Miglyol®812 to the carrier, i.e. preparation of NLC formulations, a depression of the melting point was observed. The decrease of the onset temperature is dependent on the concentration of the oil in the carrier [164]. For these nanoparticles the difference between the onset and the melting temperatures was approximately 2ºC after one year of storage at all tested temperatures and increased to 3-4ºC after two years.

4.1.4.3.2 X-ray diffraction analysis

Figs. 4.12 and 4.13 show the X-ray diffraction patterns of Dynasan®116-based SLN and NLC dispersions, respectively, recorded after three months and one year of storage at room temperature. The SLN samples show the well known scattering peaks of Dynasan®116, indicating that the lipid matrix of such carriers has a crystalline character (Fig. 4.12). Upon crystallization of tripalmitin nanoparticles the wide-angle reflections of the α modification appear first. Clotrimazole did not change the X-ray patterns of the lipid. Only a slight decrease in peaks intensity was observed after one year of storage at room temperature (Fig. 4.12, right, lower graph).

X-ray diffraction studies confirm the results obtained by DSC analysis. Concerning NLC formulations (Fig. 4.13), no peaks were recorded after running the samples indicating the presence of a more amorphous state. Also in NLC formulations the presence of drug did not influence the rearrangement of fatty acid chains in the lipid matrix.

These data emphasize the assumption of the incorporation of clotrimazole in molecularly dispersed form in between the fatty acid chains of the highly mobile liquid crystalline α modification of the loaded SLN and NLC.

After one year of storage at room temperature also D116NLC_Co showed a decrease in scattering intensity with increasing of a small peak corresponding to the α modification of Dynasan®116. This result indicates that polymorphic transformations occurred during storage time with increasing the solid fraction of the lipid matrix, as also reported by DSC analysis (Table XII).

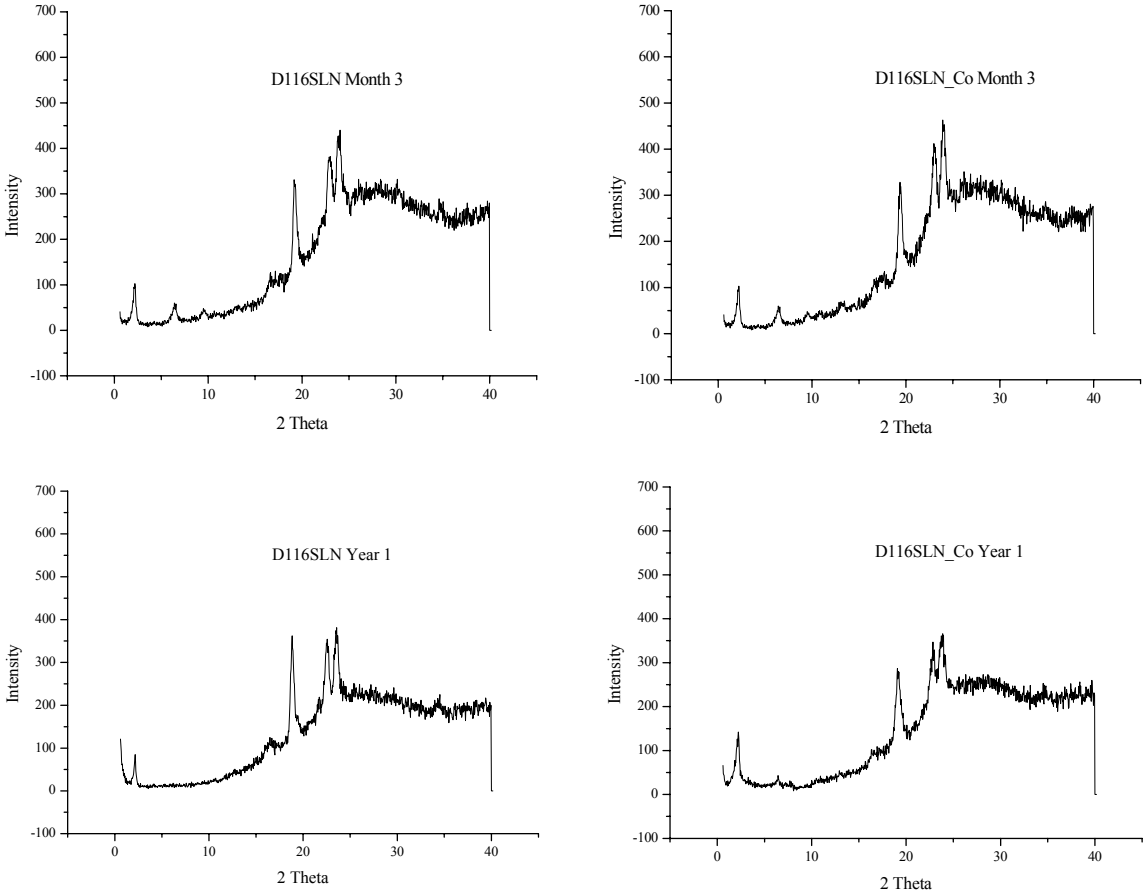

Fig. 4.12: X-ray diffraction patterns of aqueous Dynasan®116-based SLN dispersions recorded after 3 months and 1 year of storage at room temperature.

To summarise, there were no major effects on the crystallization temperature neither remarkable differences in the time-course of polymorphic transitions after crystallization of the triacylglycerols formulated as SLN systems from three months to one year of storage (Fig.4.12). Upon fast cooling from the melt, these dispersions form an uncommon type of α modification that displays only a very weak small-angle reflection indicating poor ordering between triacylglycerol layers. Upon subsequent cooling, crystallization starts only when the critical crystallization temperature for emulsified tripalmitin is reached [303]. Both drug-free

and drug-loaded SLN dispersions display wide-angle reflections at approximately 0.46, 0.385 and 0.37 nm typical of the stable β modification of triacylglycerols.

The size dependence of polymorphic transitions after recrystallization has been previously investigated for dispersions of tripalmitin [133, 298, 321]. It has been reported that recrystallization proceeds via α modification in all dispersions, and the rate of transition into the stable β modification increases with decreasing particle size.

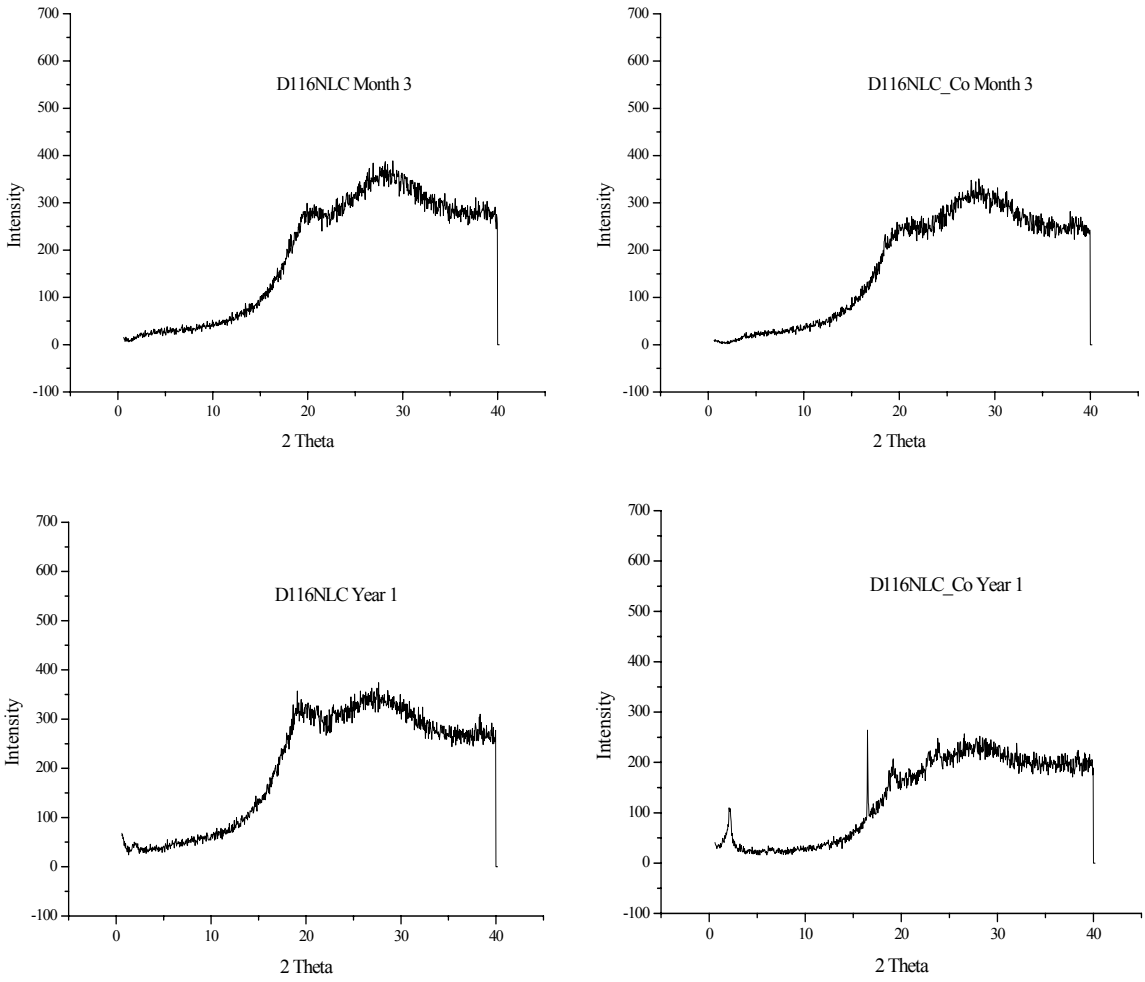

Fig. 4.13: X-ray diffraction patterns of aqueous Dynasan®116-based NLC dispersions recorded after 3 months and 1 year of storage at room temperature.

The polymorphic behaviour has also been studied for the samples at 4ºC and at 40ºC. Fig. 4.14 and 4.15 show the Dynasan®116-based SLN and NLC dispersions, respectively, recorded after three months of storage at 4ºC and at 40ºC.

The intensity of the WAXS reflections of the dispersions depended highly on the crystallization conditions. The transition kinetics of the dispersed triacylglycerols differed considerably between 4ºC and 40ºC. At higher temperatures of storage the transformation into

the stable β modification was not complete within the time scale of the experiment but the samples reached a quasi-equilibrium. Dispersions at 40ºC usually retained a higher amount of α modification than those at 4ºC. The storage at low temperatures (4ºC) increased the crystallinity of both SLN and NLC dispersions, as already reported from the DSC data. At the time of the experiments, all dispersions displayed a X-ray diffraction pattern characteristic of the stable β modification.

Concerning the SLN formulations (Fig. 4.14), the observed reflections (α, β' and β) were stronger than the samples stored at 25ºC (Fig. 4.12), meaning that polymorphic transformations occur faster both at 4ºC and at 40ºC. In contrast, in the NLC formulations (Fig. 4.15) the thermodynamic unstable α form observed at 25ºC (Fig. 4.13), which seems not to contain a highly ordered layered structure, transforms into the regular one under refrigeration conditions. Only slightly differences have been observed between drug-free and drug-loaded formulations. NLC formulations stored at 40ºC during three months remained completely in the amorphous state, whereas for SLN and NLC stored at 4ºC and SLN at 40ºC only minor reflections of the α modification were observed upon crystallization.

Different storage conditions led to differences in the matrix structure of the resulting nanoparticles. Slow cooling to room temperature yielded the common α form with its strong small- and wide-angle X-ray reflections, but an uncommon form with an extremely weak reflection was observed upon rapid cooling to refrigerator temperature.

Formation of the characteristic layered structure of triacylglycerol crystals seems to be hampered under these conditions as also reflected in the spherical shape of SLN observed by SEM (Fig. 4.2) one week of storage at room temperature. Once the uncommon α form still gives a strong wide-angle reflection, the triacylglycerol chains must still be ordered in the particles. This could result from a highly mosaic structuring of the triacylglycerol matrix. The high degree of disorder may impair recrystallization into the stable β form upon rapid heating. Rearrangement of the triacylglycerol molecules into the common α form can be induced by slow heating of the dispersion. The α crystals obtained under both rapid and slow crystallization regimes differ in shape and also have a distinctly different shape from that of β crystals. Polymorphic transitions in triacylglycerol nanocrystals are thus not only associated with molecular rearrangements but may also lead to alterations in general matrix structure and overall shape of the nanoparticles.

The molecular reorganization during polymorphic transitions is accompanied by pronounced alterations of the matrix structure and the particle shape. Such processes may be very

important for the physical stability of the colloidal state of triacylglycerol nanoparticles and also for their loading capacity for model drugs.

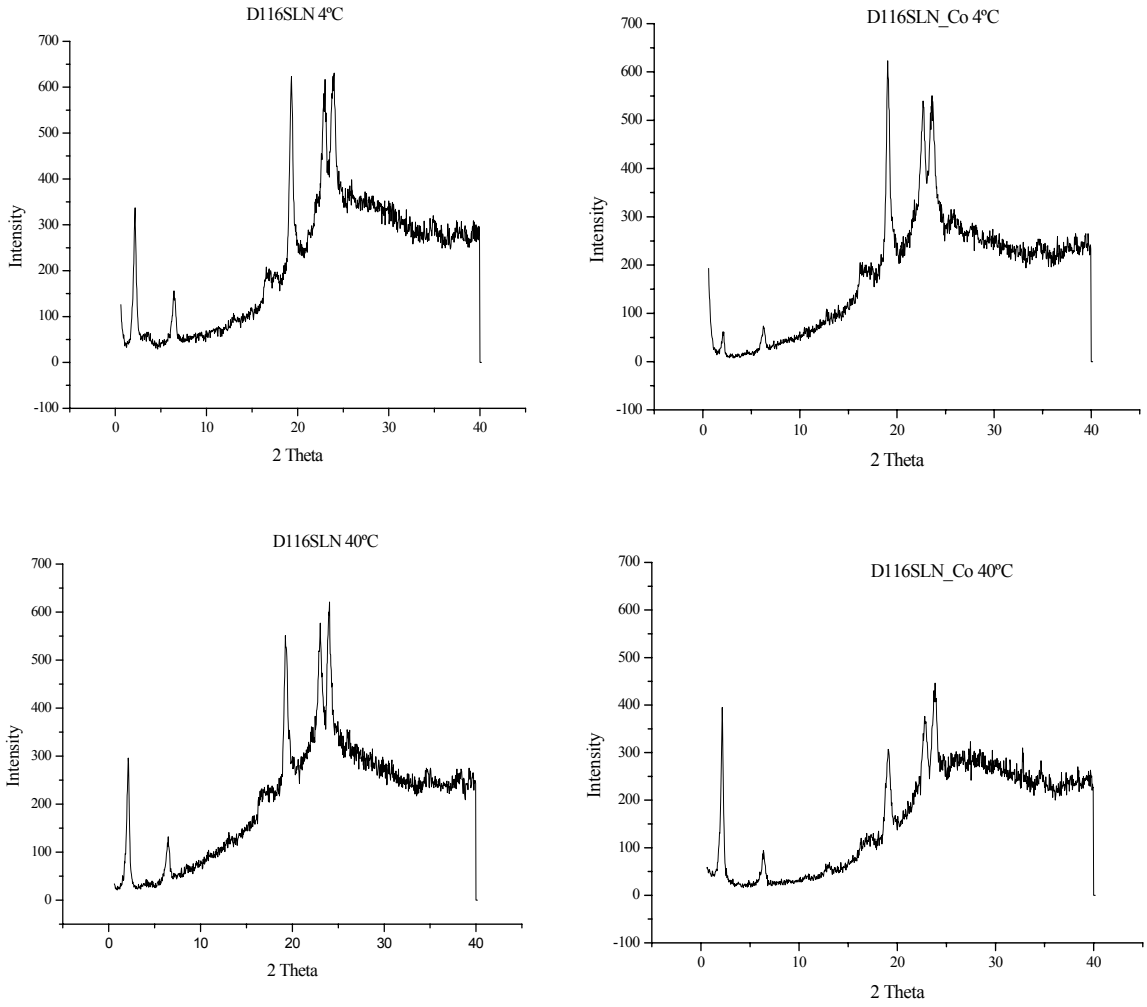

Fig. 4.14: X-ray diffraction patterns of aqueous Dynasan®116-based SLN dispersions recorded after 3 months of storage at 4ºC and at 40ºC.

DSC and X-ray diffraction studies of aqueous Dynasan®116-based SLN and NLC dispersions indicate that clotrimazole does not recrystallize even at lower temperatures of storage (4ºC). The almost constant crystallization temperature in these dispersions indicates a homogeneous nucleation process, which is not dependent on the presence of Miglyol®812. In many dispersions the triacylglycerols crystallize at distinctly higher temperatures pointing that is a heterogeneous nucleation [331]. In such cases, the crystallization event is often accompanied by a small pre-transition at even higher temperatures. A few dispersions also display small additional crystallization events above 40ºC, which are in the region of the crystallization temperature of the bulk material [133], and may indicate the presence of a coarse material in

the dispersion [331]. The observation that crystallization may occur at elevated temperature when the dispersions are prepared with specific stabilizers indicates an interaction with the surfactant layer. This phenomenon is usually referred to as surface heterogeneous nucleation.

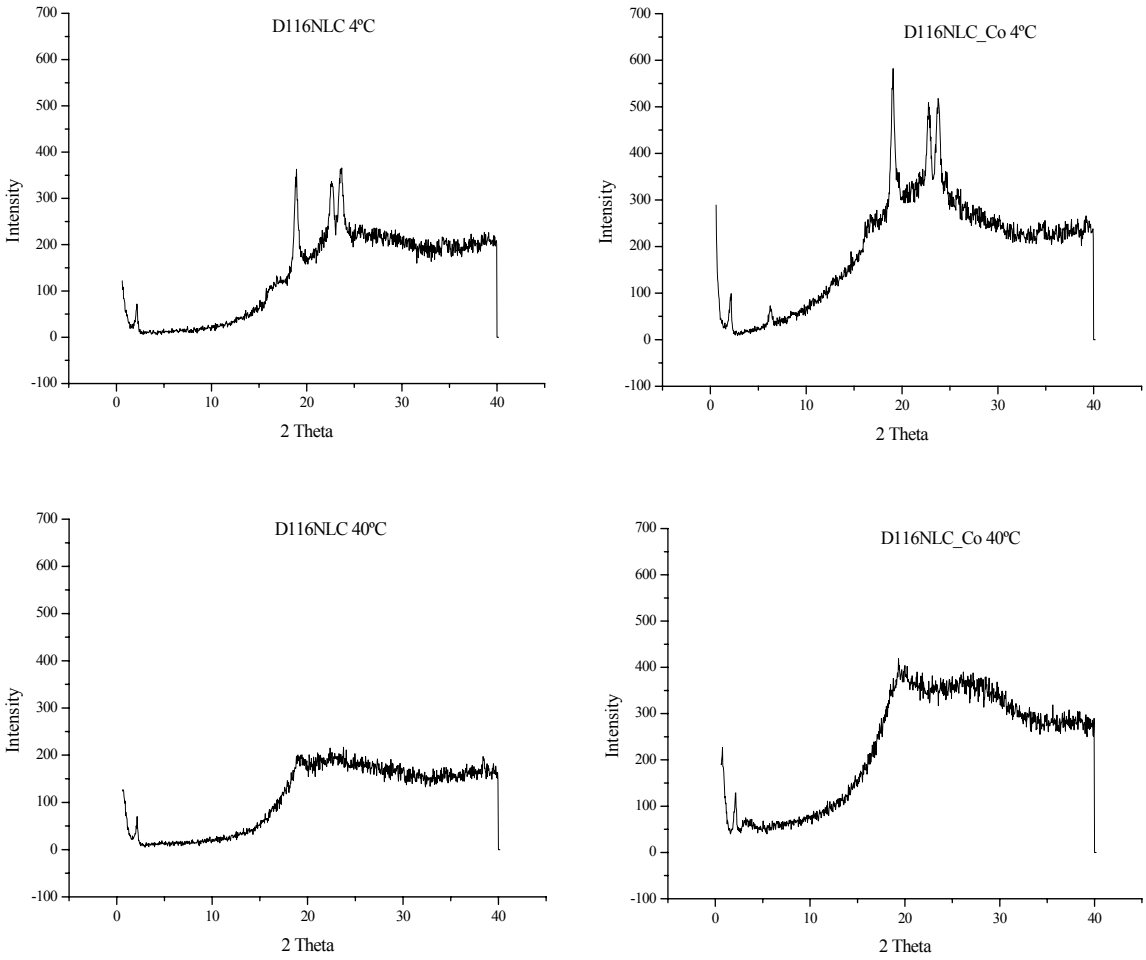

Fig. 4.15: X-ray diffraction patterns of aqueous Dynasan®116-based NLC dispersions recorded after 3 months of storage at 4ºC and at 40ºC.

The polymorphic transitions have been monitored continuously by WAXS experiments. It has been already observed that non-ionic surfactants usually seem to promote the transition into the stable β polymorph [331]. The crystallization tendency of the particles increases with the length of the saturated hydrophobic chain of the stabilizer. In contrast, unsaturated longer chain surfactants do not have an increasing effect on the crystallization temperature. These observations together with the occurrence of a pre-transition in many dispersions with increase crystallization, suggest that the crystallization promoting effect of certain surfactants is caused by an ordering process of the surfactant molecules in the stabilizer layer.

4.1.5 Assessment of the chemical stability of clotrimazole in SLN and NLC

The chemical stability of clotrimazole in the aqueous dispersions of SLN and NLC has been assessed by HPLC analysis, in comparison to a reference emulsion prepared using Miglyol®812 as internal phase stabilized with Tyloxapol® in the same concentration (5%, m/m).

Fig. 4.16 depicts the percentage of clotrimazole recovered from D116SLN_Co and from D116NLC_Co, in comparison to the reference emulsion (RefEm_Co), during two years of storage at three different temperatures. Those values have been determined against an appropriate calibration curve (Fig. 3.10, Chapter 3) obtained using acetone as organic solvent for the formulations.

Immediately after production (day 0) the percentage of drug recovered was 91.7% for D116SLN_Co and 98.7% for D116NLC_Co. During shelf life, the amount of drug recovered has decreased.

The prepared reference emulsion showed comparable particle size, i.e. the mean size obtained by PCS was 196 nm with a PI of 0.121. It is clearly visible the effect of drug protection of lipid nanoparticles in comparison to the reference emulsion. While the reference emulsion contained clotrimazole dissolved in the oil in the same concentration as the lipid nanoparticles formulations, in these latter (SLN and NLC) the drug has been immobilized in the solid core, i.e. in between the fatty acid chains.

Comparing both nanoparticle systems, NLC depicted a higher ability to stabilize this drug during storage time at three different temperatures. In agreement to the DSC and X-ray studies, which have shown the occurrence of polymorphic transformations especially in SLN systems, these changes may be related to drug expulsion from the system. However, these results are quite promising once after two years approximately 90% of drug has been detected by HPLC analysis. SLN based on relatively high ordered lipids have been first prepared for the incorporation of clotrimazole. A content of partial acylglycerols (Miglyol®812) in a liquid core favours successfully the drug inclusion and avoids its expulsion, as described previously [33]. Concerning the different storage temperatures, no major differences have been recorded. Higher amount of drug recovered has been obtained for all formulations stabilized at 25ºC, i.e. 98.5% one day after production and approximately 95% after two years. The lower values were obtained at 40ºC, i.e. approximately 86% after two years, as expected because of the higher lipid disorder of both SLN and NLC matrices at this temperature of storage.

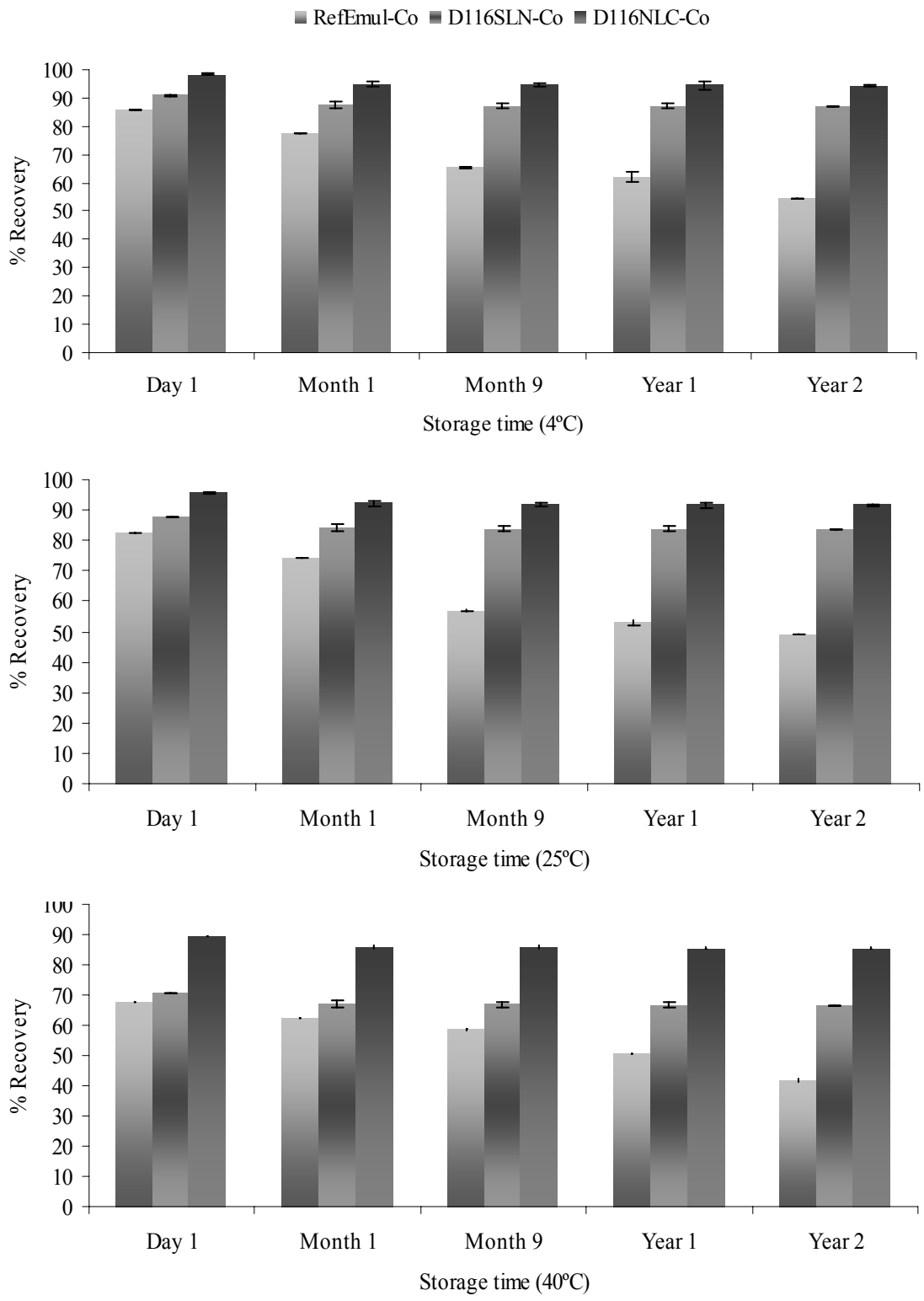

Fig. 4.16: Percentage of drug recovered during two years of storage at 4ºC, 25ºC, 40ºC for D116SLN-Co and D116NLC-Co in comparison to a reference emulsion.

4.1.6 Rheological analysis of Dynasan®116-based lipid nanoparticles

Pharmaceutical dosage forms intended for topical and dermatological administration of drug substances are rheologically characterized by structural parameters such as the dynamic storage modulus (G'), being nearly independent on the angular frequency, and the values of the loss modulus (G"), which are at least one order of magnitude lower than the G' values. However, those formulations may also be rheologically characterized as weak structures, where the mechanical spectra of such formulations are slightly different from those of conventional gels in several aspects. There is a small linear viscoelastic region, G' and G" moduli are frequency dependent and at the maximum, the G' values are higher by one order of magnitude compared to the G" values [332].

Previously to oscillatory testing, the linear viscoelastic region for all different Dynasan®116-based lipid nanoparticles has been determined by a strain sweep test. The complex modulus (G*) has been measured as a function of strain at a constant frequency [333]. All measurements have been carried out in the regime of linear viscoelasticity at a stress amplitude of 5 Pa, i.e. where the material parameters are independent on the applied stress.

Once aqueous SLN and NLC dispersions are not isotropic solutions, their viscoelastic parameters are not independent on the applied shear rate [332], indicating a rheological behaviour completely different from Newtonian systems. Therefore, these studies have been performed immediately after the production of the formulations, at different storage conditions and during shelf life.

4.1.6.1 Immediately after production

On the day of production of Dynasan®116-based lipid nanoparticles, the drug-free and drug-loaded dispersions have been analysed applying a frequency from 0.1 to 10 Hz (Figs. 4.17 and 4.18).

From the results presented in Fig. 4.17, the effect of the presence of drug is perfectly clear. Without clotrimazole the dispersions depicted a G' much than the G" values, which means that the system is more elastic than viscous in the investigated frequency range. Both parameters show weak dependence on the applied frequency. On the other hand, the complex viscosity depends very much on the frequency, i.e. decreases with increasing the frequency. With regard to the drug-loaded systems, G' is also higher than G" however their values are much smaller than drug-free systems. Also the complex viscosity showed to be dependent on the

frequency. Based on the values of the loss tangent, both formulations (D116SLN and D116SLN_Co) could be classified as elastic (tan δ < 1) [334]. The smaller the ratio G"/G' (tan δ), the more elastic is the rheological behaviour [335].

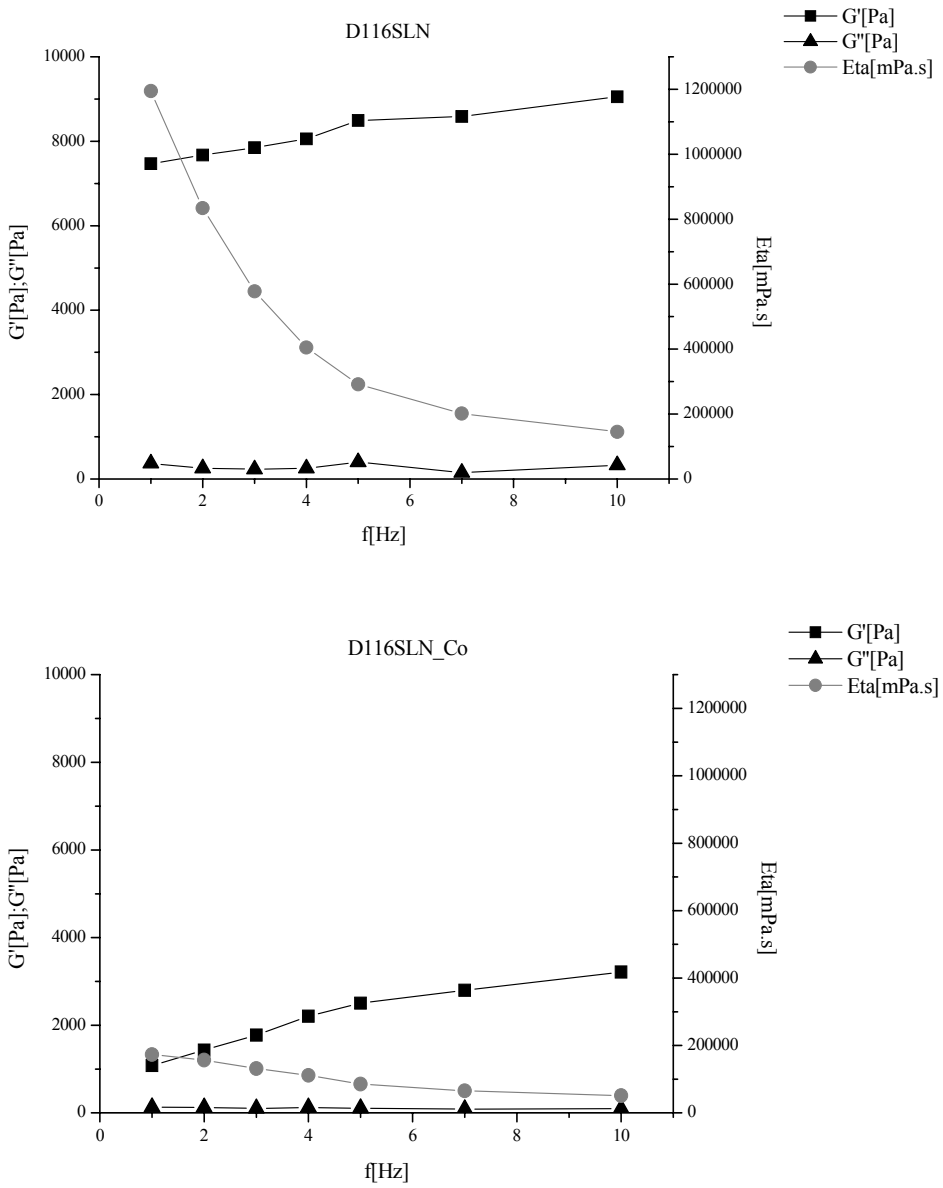

Fig. 4.17: Storage modulus (G'), loss modulus (G'') and complex viscosity (Eta) of aqueous Dynasan®116-based SLN dispersions as a function of frequency, recorded immediately after production under a constant stress amplitude of 5 Pa.

A completely different rheological behaviour as a function of the frequency could be observed for NLC dispersions. Looking at the values of G' and G" they are much smaller than the ones registered for SLN dispersions, which is due to the presence of Miglyol®812 inside the particles. Dynamic rheological experiments have shown for NLC formulations without drug a weak structure where the storage modulus and the loss modulus are almost parallel and

frequency dependent. When comparing both SLN and NLC formulations, the increase in solid lipid content (20% in SLN and 14% in NLC) caused a significant increase of the elastic modulus (G'). In contrast to this, the viscous modulus was not significantly different.

The presence of clotrimazole in NLC formulations (Fig. 4.18, lower) increased the differences registered between both moduli, revealing a more elastic system than the drug-free NLC formulations (Fig. 4.18, upper). In D116NLC, the complex viscosity and both moduli are much lower, which exhibits the much weaker structure of the system having a more liquid character.

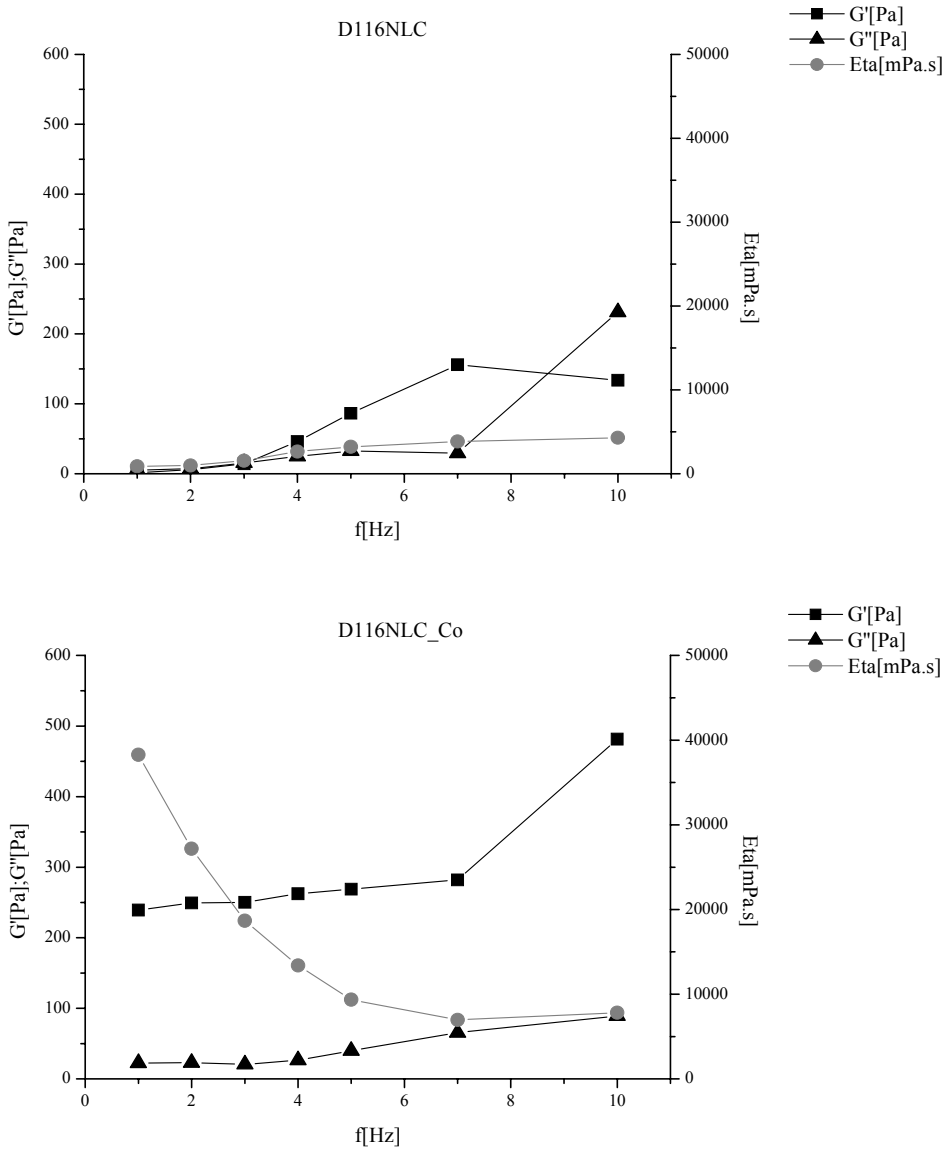

Fig. 4.18: Storage modulus (G'), loss modulus (G'') and complex viscosity (Eta) of aqueous Dynasan®116-based NLC dispersions as a function of frequency, recorded immediately after production under a constant stress amplitude of 5 Pa.

G' is a measure of the recoverable energy stored elastically in the system, whereas G" is a measure for the energy dissipated as viscous flow representing the real and imaginary parts of the complex dynamic shear modulus, respectively. A comparison of storage modulus (G') and loss modulus (G") without and with clotrimazole shows significant differences. In both situations, the elastic modulus G' dominates the viscous modulus G", and they are not in the same range when comparing samples with and without drug. An interesting observation is the fact that for SLN formulations the drug maintains the elastic properties of the systems, while the drug-free NLC formulations become more viscous at the end of the assay, i.e. when reaching the frequency of 10 Hz (tan $\delta > 1$). This is a characteristic of a lower structured system of these latter.

Particle size is known to be an important rheological variable of dispersed systems [336]. Dispersions with a lower particle size will have preferentially a more elastic behaviour in comparison to the ones with greater particle average. The greater mean size and the widest size distribution will preferentially show more viscous properties. In the present case, the developed aqueous SLN and NLC dispersions were comparible in size, i.e. mean particle size ranged between 200 and 250 nm, which contribute for the increase of the elastic component.

4.1.6.2 At different temperatures of storage

Knowledge of the effect of storage conditions on the rheological properties of aqueous SLN and NLC dispersions can be very useful in order to correlate experimental observations with the system's structure. Viscoelastic parameters have been evaluated after one month of storage at three different temperatures (4º, 25º and 40ºC), under a constant stress amplitude of 5 Pa. Table XIII depicts the obtained results.

All viscoelastic parameters, i.e. the system's strength, are strongly dependent on the temperature that samples have been stored. Looking at the values of the structural parameters G' and G", after applying a frequency range between 1 and 10 Hz, in all storage temperatures G' is always greater than G" for samples without clotrimazole, which indicates that either the systems are more structured or have a compact network. In all situations, G' showed dependency upon the frequency, which increased during the assay. The higher complex viscosity values have been recorded for samples stored at 25ºC. Interesting was the fact that samples stored at room temperature showed a decrease in complex viscosity during the assay, which is typical of pseudoplastic materials, while at 4ºC and at 40ºC those values increased.

The G' value increased enormously for samples stored at 25ºC. As expected, also the samples stored at 4ºC and at 40ºC showed G' values higher than those of G" values. Both modulli are almost temperature-dependent and parallel to each other.

Table XIII: Storage modulus (G'), loss modulus (G'') and complex viscosity (Eta) of aqueous Dynasan®116-based SLN and NLC dispersions as a function of frequency, recorded after one month of storage at three different temperatures, under a constant stress amplitude of 5 Pa.

Sample	Storage temperature	f [Hz]	G' [Pa]	G'' [Pa]	Eta [mPa.s]
D116SLN	4ºC	1	50	48	11000
		10	1210	324	20000
	25ºC	1	4050	417	647667
		10	14720	657	234800
	40ºC	1	23500	1670	652000
		10	40900	522	3750000
D116SLN_Co	4ºC	1	3	3	636
		10	50	82	1520
	25ºC	1	16300	618	2597333
		10	30123	630	479333
	40ºC	1	2	2	388
		10	140	34	2290
D116NLC	4ºC	1	3	13	2110
		10	2590	289	41500
	25ºC	1	1061	84	169402
		10	1664	199	26950
	40ºC	1	3	8	1380
		10	198	194	4410
D116NLC_Co	4ºC	1	3	5	883
		10	614	228	10400
	25ºC	1	114530	19316	18498208
		10	129007	13932	2065460
	40ºC	1	0	2	300
		10	215	59	3550

Under higher temperatures, the system might undergo phase transitions, which are responsible for the weak structure revealed by the rheological analysis. In addition, also samples at 4ºC are more sensitive since both moduli are smaller than those collected for samples at 25ºC.
These results are in accordance to the polymorphic behaviour that lipid nanoparticles suffer under different storage conditions. The G' and G" do not have the same values in all storage temperatures. They approach each other prior to reaching the critical temperature and after that their modulus values separate again. This indicates that the formulations suffer a minor structural modification, even below the critical temperature.

4.1.6.3 During shelf life

Concerning the aging, the rheological results presented in this section have been collected during one year of storage at room temperature (Table XIV). The results recorded within a period of three months after the sample preparation are denoted as the initial gel stage [332]. Knowledge about the stability of the formulations with respect to time is essential for the characterization of the physical stability of the colloidal systems and the consistency of the aqueous dispersions, as well as for the possibility of their industrial application.
The results shown in Table XIV indicate that all the viscoelastic parameters (G', G" and complex viscosity) are affected identically by aging. It can be inferred on the basis of the elastic modulus that the older formulations always display higher values of all mechanical moduli than those at the initial stage (three months). The values recorded for G' were greater by one order of magnitude compared with the G" values for the same formulation at its initial stage. The rheological results may be understood in terms of a very slow kinetics that takes place in the system. The existence of higher values of all the mechanical parameters may indicate that the material has a higher solid-like character than the freshly prepared formulation and that this solid-like character is due to a substantial enhancement of the dispersion strength by aging. The modification looks to be depent on the sample composition, i.e. SLN and NLC, with and without clotrimazole. Moreover, an inflexion in the viscoelastic parameters was observed after one year of storage, which may be related to disruption of the structure. Depending on the nature of the dispersed lipid phase (SLN or NLC) the rheological parameters became significantly different with storage time. While at low frequency both moduli are very small, with increasing the applied frequency they become significantly different showing their dependence on the applied frequency. Concerning the viscosity, this parameter increased with storage time during the first three months but showed a decaying

after one year. In order to overcome this problem, the aqueous SLN and NLC suspensions need to be incorporated into semi-solid systems to have a suitable consistency for topical application.

Table XIV: Storage modulus (G'), loss modulus (G'') and complex viscosity (Eta) of aqueous Dynasan®116-based SLN and NLC dispersions as a function of frequency, recorded after seven days (D7), three months (M3) and one year (Y1) of storage at room temperature, under a constant stress amplitude of 5 Pa.

Sample	Storage time	f [Hz]	G' [Pa]	G'' [Pa]	Eta [mPa.s]
D116SLN	D7	1	7470	370	1194486
		10	9054	329	145103
	M3	1	9160	1195	1469667
		10	22910	903	365167
	Y1	1	2	4	709
		10	567	281	10100
D116SLN_Co	D7	1	1078	129	173107
		10	3214	96	51273
	M3	1	4880	271	777533
		10	9258	134	147100
	Y1	1	2	2	419
		10	57	22	980
D116NLC	D7	1	2	5	892
		10	134	231	4306
	M3	1	4173	516	668333
		10	9833	491	156933
	Y1	1	1	1	132
		10	164	73	2850
D116NLC_Co	D7	1	239	23	38275
		10	481	89	7820
	M3	1	301	55	48792
		10	489	123	8040
	Y1	1	1	1	126
		10	77	84	1820

4.2 Development and characterization of ketoconazole-loaded SLN and NLC

The use of lipid-based formulations for topical administration of ketoconazole is well known [337]. Some examples are Nizoral® cream and Nizoral® Shampoo. However, until now formulations intended for drug targeting, i.e. under the micrometer range have not been yet developed. Colloidal carrier systems for the delivery of ketoconazole have been already developed applying the so-called SolEmuls® technology [338], which is suitable for the production of emulsions of slightly or poorly soluble drugs [339]. The aim of the present section is the assessment of the use of lipid nanoparticles intended for topical administration of ketoconazole.

For the present study four different formulations have been developed, containing two of them 0.750% (m/m) of ketoconazole. Table XV shows their composition (the symbols C888 and Ke stand for Compritol®888 ATO and ketoconazole, respectively). Compritol®888 ATO has been selected as the solid lipid for ketoconazole entrapment after screening the solubility of this drug in several lipids with sufficient high melting point. The selection of α-tocopherol as liquid lipid for NLC preparation was also based on solubility studies.

Table XV: Composition of Compritol®888 ATO-based SLN and NLC formulations (%, m/m).

Formulation composition	Formulation code			
	C888SLN	**C888SLN_Ke**	**C888NLC**	**C888NLC_Ke**
Compritol®888	15.000	14.250	10.500	10.125
α-Tocopherol	-	-	4.500	4.125
Poloxamer®188	2.500	2.500	2.500	2.500
Sodium deoxycholate	0.125	0.125	0.125	0.125
Ketoconazole	-	0.750	-	0.750
Water ad	100	100	100	100

For the production of NLC formulations the optimized ratio between Compritol®888 ATO and α-tocopherol has been determined after screening different proportions of both lipids by DSC studies to evaluate the absence of free oil in the melted mixtures. No free oil has been detected after running the heated bulk mixtures of solid and liquid lipids until -50ºC. Mixtures of both lipids at different ratios have been melted at 85ºC and further analysed by DSC. Fig.

4.19 depicts the melting and the onset temperature values of bulk Compritol®888 ATO with increasing amounts of α-tocopherol from 10% to 40% (m/m).

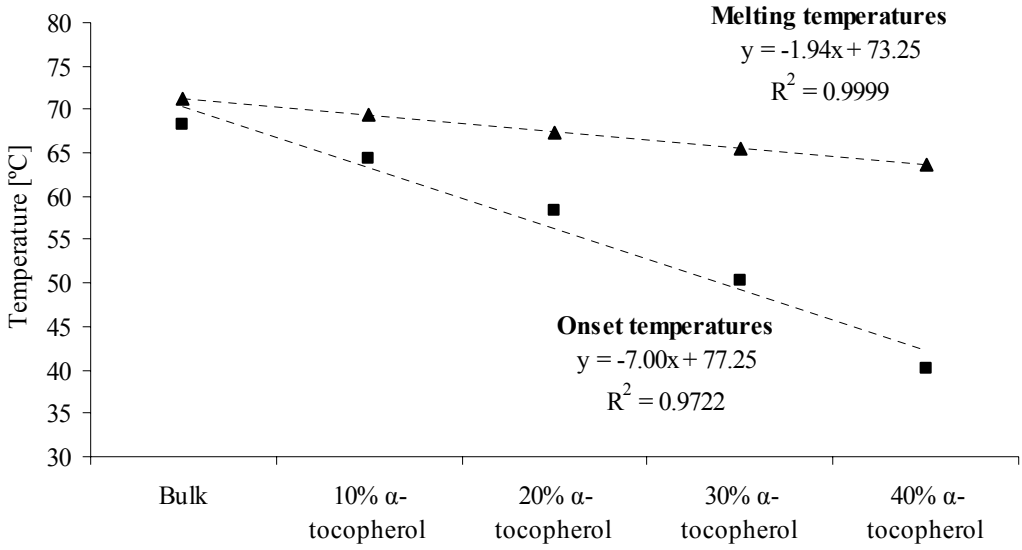

Fig. 4.19: Melting temperatures (= peak maximum) and onset temperature values of bulk lipid (Compritol®888 ATO) with increasing amounts of liquid lipid (α-tocopherol) from 10% to 40% (m/m).

The melting process of the bulk material took place at 71.3ºC (peak maximum), with an extrapolated onset of the melting process at 68.3ºC. The differences between the onset and the maximum temperatures can be taken as a measure of the width of the peak and in this case it was approximately 3. By adding α-tocopherol to Compritol®888 ATO, the melting point of the melted mixtures of both lipids was obviously depressed. With 10% of α-tocopherol the difference between the temperature values was 5.1 and increased to 23.3 when the mixture contained 40% of the oil. The width of the melting peak gives insights about the structure of the lipid mixture. In fact, the increase of the oil content in the lipid mixture will destroy the crystalline structure of the solid lipid, being dependent on the concentration. In Fig. 4.19 it is clearly visible the increase of "impurities" once the onset temperature decreases significantly. This is due to the creation of a more amorphous material (mixture of oil and solid lipid), in comparison to the pure solid lipid (Compritol®888 ATO). The obtained correlation coefficient of the melting curve was R^2 = 0.9999 and of the onset curve was R^2 = 0.9722. A lipid phase containing 30% of α-tocopherol has been selected once the melting point of the mixture was registered at 65.5ºC with an onset at 50.3ºC, which is higher than 40ºC.

It has been previously reported that when using complex acylglycerols such as hard fats as matrix for SLN, incorporation of lipophilic drugs, such as ketoconazole should be facilitated [340]. However, these complex hard fats lead to the formation of supercooled melts instead of solid nanoparticles. Even if a solid core is formed when solidified at room temperature, the particles obtained will melt at body temperature. Therefore, these lipids might not be suitable for controlled release purposes. The ability to include host molecules in the lattice of crystalline lipids is often limited whereas liquid oils normally show considerable higher solubility for lipophilic drugs [164]. Mixtures of liquid and solid lipids are not restricted to the semi-synthetic materials used to prepare lipid nanoparticles, but they can be found as well in naturally occurring products such as milk, cream or cocoa butter [341]. Similarly, in this study a portion of the lipid matrix of SLN has been replaced by liquid oil (α-tocopherol).

The concept was to develop NLC, i.e. having particles with a solid matrix but also having liquid domains. NLC combine the advantages of the solid matrix, which prevents drug leakage, and of the liquid regions, which show comparably higher solubility for ketoconazole. In contrast to complex hard fats, a bulk material with sufficient high melting point (between 40ºC and 70ºC) was chosen. The mixture of solid and liquid lipid needs to melt at temperatures higher than 40ºC. Similar to most hard fats, the chosen Compritol®888 material consists of mono- (15%), di- (50%) and triacylglycerols (35%) showing slight emulsifying properties to the lipid (HLB valued of 2) [164]. This long chain acylglycerol (C_{22}) was mixed with varying amounts of α-tocopherol, where the model drug ketoconazole showed high solubility. The selection of this oil was due to its good miscibility with Compritol®888. After DSC analysis of the different mixtures a ratio of 70:30 has been selected for the production of NLC, once it was the highest amount of liquid oil possible to incorporate into Compritol®888 nanoparticles and maintaining an onset temperature higher than 40ºC. In addition, the oil leads to higher amount of solubilized ketoconazole.

4.2.1 Assessment of the physical stability of the developed formulations

The particle electrical charge and the size parameters of the developed formulations have been evaluated immediately after production and they have been monitored during one year of storage at two different temperatures (4ºC and 25ºC). The systems stored at room temperature (25ºC) have also been evaluated concerning their protection against light exposure.

4.2.1.1 Immediately after production

Table XVI shows the zeta potential and particle size parameters of Compritol®888-based SLN and NLC formulations collected on the day of production.

Table XVI: Zeta potential and particle size parameters of Compritol®888-based SLN and NLC formulations obtained immediately after production.

Parameters		C888SLN	C888SLN_Ke	C888NLC	C888NLC_Ke
ZP (mV)		-21.9±0.2	-20.1±0.1	-20.0±0.1	-19.5±0.0
PCS (nm)		199.6±5.7	228.3±9.6	235.2±9.3	236.4±2.9
PI		0.321±0.112	0.190±0.131	0.361±0.138	0.215±0.154
LD (μm)	LD50	0.109±0.001	0.110±0.001	0.111±0.002	0.259±0.011
	LD90	0.290±0.012	0.277±0.021	0.302±0.017	0.412±0.004
	LD95	0.361±0.006	0.344±0.011	0.366±0.005	0.449±0.002
	LD99	0.484±0.012	0.466±0.025	0.474±0.023	0.522±0.002

Immediately after production, the macroscopic appearance of the aqueous dispersions was similar to milk, of low viscosity and with white colouration.

As reported previously, Compritol®888 is a partial acylglycerol, therefore it shows surface active properties. Once its use facilitates the emulsification process by forming a more rapid surfactant films, it might be related to improvements of physical stability of lipid nanoparticles [209]. Replacing 30% of solid lipid by oil, the percentage of mono- and diacylglycerols is reduced. Thus, increasing oil loads should tend to broaden the size distribution and reduce the stability. Using a surfactant/co-surfactant system for stabilization of lipid particles, a mean particle size lower than 250 nm was obtained with a PI lower than 0.400. LD measurements revealed basically similar sizes and size distributions with LD50% values around 0.100 μm, except for C888NLC_Ke with approximately 0.260 μm. The LD99% was lower than 0.550 μm for all formulations. The immediate influence of oily constituents on the production process was, as expected obviously low. In contrast, ketoconazole influenced the size parameters and slightly decreased the ZP values. However, those differences were not significant.

Sodium deoxycholate used as co-surfactant in combination with Poloxamer®188 was shown to prevent gelation. Bile salts are highly mobile ions and therefore are supposed to support the emulsifying role of comparably slowly moving poloxamers by stabilizing the freshly

generated surfaces during the homogenization process [210]. This protective effect was attributed to the introduction of charges in the carrier surface as could be demonstrated by measurements of ZP [342]. The employed amount of bile salt was below its critical micellar concentration (2.4 mmol/dm^3 at 298 K) [343], in order to provide for the immediate availability of ions for surface stabilization. Gelation seems to be correlated with specific interactions between the surfactant and co-surfactant molecules [256]. In such systems the emulsifier molecules can partition between different possible locations. The co-surfactant is in this case ionic and of very low MW. It is assumed that the use of co-surfactants serves as reservoir of stabilizing agent which is immediately available as soon as recrystallization of the lipid takes place [344]. These results suggest that the high aqueous solubility in combination with the formation of highly dynamic micelles of both surfactants are the major requirements to stabilize the dispersed state during the re-solidification step of the lipids [267].

4.2.1.2 At different temperatures of storage

Preliminary experiments of the present work showed that lipid nanoparticles containing ketoconazole were sensitive to light exposure and to high temperatures of storage. The physical stability at 4ºC and 25ºC, as well as at 25ºC under darkness, performed three months after production of the aqueous dispersions is therefore reported here. Table XVII shows the obtained results.

Measurements of particle sizes three months after production revealed huge differences between the developed formulations stored under different conditions. After 90 days of storage, ketoconazole-loaded SLN formulations yielded a mean particle size between 210 and 260 nm. It was possible to detect a pronounced increase in the mean particle size and PI of NLC formulations. Ketoconazole-free SLN stored at 25ºC revealed a mean particle size higher than 3 μm.

The pH values of all developed formulations oscillated between 5.5 and 6.0. The ZP values of cold stored Compritol®888 ATO nanoparticles were lower than of those stored at room temperature (25ºC). The ketoconazole-loaded NLC formulations stored at room temperature under light exposure showed a positive ZP value in contrast to the sample protected from light. PCS is limited to detection of particles undergoing Brownian motion, and particles larger than approximately 3 μm are therefore not detectable [292]. However, the presence of microparticles and/or liquid lipid droplets could be determined by LD measurements. Drug-loaded SLN formulations stored at both temperatures were fitted to a perfect log-normal

distribution by cumulative analysis. In contrast to SLN stored at 4ºC, the storage at 25ºC slightly increased the particle size; however, protection against light exposure could avoid particle growth. Concerning NLC formulation stored at 4ºC, the size distribution shifted to bigger particles showing a broadened distribution pattern. In comparison to SLN, the observed destabilization of NLC seems to result from the presence of a liquid component inside the lipid matrix of this carrier, i.e. α-tocopherol, which might cause aggregation of the particles. Furthermore, in contrast to ketoconazole-loaded NLC under light exposure, drug-loaded SLN showed a purple colour. This result shows the effect of the antioxidant α-tocopherol used as matrix material of glycerol behenate-based NLC.

Table XVII: Zeta potential and particle size parameters of Compritol®888-based SLN and NLC formulations stored at different temperatures and obtained three months after production. (25ºC^{dark} stands for samples containing ketoconazole stored at 25ºC under light protection).

Sample	Storage temperature	ZP (mV)	PCS (nm)	PI	LD (µm)	
					LD50	LD90
C888SLN	4ºC	-21.6±0.5	211.6±4.3	0.159±0.080	0.11±0.00	0.49±0.00
	25ºC	-10.7±1.6	> 3 µm	1.0±0.0	19.27±0.61	174.65±16.51
C888SLN_Ke	4ºC	-24.0±1.7	212.3±7.4	0.157±0.059	0.11±0.00	0.46±0.00
	25ºC	-18.3±0.5	214.1±7.2	0.241±0.048	0.11±0.00	0.48±0.00
	25ºC^{dark}	-17.6±0.1	261.9±9.3	0.278±0.050	0.14±0.04	0.56±0.03
C888NLC	4ºC	-17.4±0.8	> 3 µm	1.0±0.0	27.12±1.49	331.55±86.30
	25ºC	-14.4±0.8	244.9±11.6	0.282±0.050	2.89±1.63	60.92±2.81
C888NLC_Ke	4ºC	-22.3±0.7	> 3 µm	1.0±0.0	39.13±2.50	490.85±46.85
	25ºC	2.8±1.5	> 3 µm	1.0±0.0	4.68±2.27	51.30±1.48
	25ºC^{dark}	-5.9±0.3	> 3 µm	1.0±0.0	12.12±0.39	35.57±5.61

The good stability of SLN at 8ºC in the dark was also pointed out for lipid nanoparticles prepared by HPH, as the introduction of energy to the system (temperature, light) leads to particle growth and subsequent gelation [257].

As shown in Table XVII, the ZP of ketoconazole-loaded NLC stored at 25ºC in light and dark was close to zero. This lack of electrostatic repulsion can explain the aggregation of these particles. However, the ZP of ketoconazole-loaded NLC stored at 4ºC is around -20 mV, i.e. similar to the values of the various SLN which proved to be physically stable [257]. From the literature, a minimum ZP of greater than -60 mV is required for excellent stability, and of

greater than -30 mV for good physical stability [345]. Nevertheless, a ZP of -20 mV is just below the critical value. This clearly indicates the effect of the lipid matrix material, i.e. the admixture of α-tocopherol. Particle aggregation and even gel formation have been described by lecithin-mediated effects [256], a similar effect is assumed in this case. It should be pointed out that the final formulation would be a cream loaded with SLN/NLC or a viscosity enhanced particle dispersion (gel). In these systems, even physically unstable, SLN and NLC show a high stability [60]. From this, the size obtained for NLC formulations does not make them necessarily unstable for a topical ketoconazole preparation.

4.2.1.3 During shelf life

Measurements for long-term stability analysis of the developed formulations have been performed one year after the production of nanoparticles and in Table XVIII those results are compared to the ones obtained after one day.

Compritol®888-based SLN and NLC formulations depicted very different long-term stabilities. Whereas the nanoparticles with no oil showed sufficient long-term stability with only slight particle growth, NLC resulted in considerable aggregation, especially the ones having drug.

Table XVIII: Zeta potential and particle size parameters of Compritol®888-based SLN and NLC formulations obtained after one day (D1) and one year (Y1) of storage at 25ºC and under light protection for samples containing ketoconazole.

Sample / Storage time		ZP (mV)	PCS (nm)	PI	LD (µm)	
					LD50	LD90
C888SLN	D1	-21.4±0.1	214.3±5.7	0.198±0.064	0.109±0.001	0.472±0.012
	Y1	-12.3±0.0	304.5±1.3	0.231±0.032	0.368±0.213	0.682±0.014
C888SLN_Ke	D1	-19.8±0.0	217.1±1.7	0.202±0.055	0.223±0.018	0.595±0.004
	Y1	-10.6±0.9	1386.8±3.2	0.992±0.124	30.482±0.157	50.781±0.073
C888NLC	D1	-16.1±0.0	712.6±19.1	0.279±0.122	0.326±0.011	0.585±0.001
	Y1	-12.4±0.2	914.3±4.2	0.716±0.314	0.836±0.176	1.923±0.013
C888NLC_Ke	D1	-7.2±0.0	238.8±9.4	0.235±0.041	0.344±0.013	0.588±0.003
	Y1	-1.6±0.0	1243.2±21.6	1.0±0.0	31.370±1.432	74.229±2.881

Due to the presence of anionic or cationic radicals in their chains, polyelectrolytes are charged macromolecules that have unique properties, because the electrostatic interactions between the charges cause repulsion-contraction of the chains [346]. At first, these polymers were used as rheology modifiers but one of the most interesting uses of these materials has been the stabilization of a wide variety of colloidal systems, including lipid nanoparticles [19]. Poloxamer®188 has been used for the stabilization of Compritol®888-based SLN and NLC and the resultant dimensions and porosity of lipid nanoparticles are also strongly linked to eventual particle agglomeration. An important factor in agglomeration is the attraction between particles, which is governed by the amount of adsorbed polymer.

There are three factors involved in the stabilization of the colloidal systems [346]: (i) the polymer conformation in the solution, (ii) the specificity of interactions between the macromolecules and the surface, whether they are of a purely electrostatic nature, or whether hydrogen bonding predominates, and (iii) the specificity of interactions between the particles.

Concerning the ZP results, although most sites at the surface of the particles are neutral, some others are usually charged, which results the creation of an ionic atmosphere surrounding the particles. Because of these charges, ions of opposite charge tend to cluster. Two regions of charge must be distinguished. First, there is a fairly immobile layer of ions that stick tightly to the surface of the colloidal particle, which may include water molecules. The radius of the sphere that captures the rigid layer, or the radius of shear, is the major factor that determines the mobility of the particle. The inner shell of charge and the outer atmosphere is called electric double layer. The potential at the slipping plane of this double layer is the ZP. As ZP tends to zero, the repulsion between the particles is minimized and they tend to collapse. As ZP tends to higher values, the system tends to be stabilized. There has been plenty of explanations for the influence of the adsorption of polyelectrolytes on different surfaces, as well as for the correlation of this adsorption to ZP and, therefore, to their stabilities. During the shelf life, the ZP decreased significantly.

Once the developed formulations have been stabilized with the same concentration of surfactant/co-surfactant system, polymer concentration does not play an important role in the increase of particle size. From Table XVIII one can draw a correlation between the presence of drug and particle size. Gelation was not macroscopically observed when using this surfactant/co-surfactant combination, however, a substantial increase in particle size has been reported by PCS and LD measurements during storage time. This phenomenon seems to be related to the crystallization of the dispersed phase which is associated with an enormous

increase of the surface area due to the formation of anisometric platelet-like particles, very well known for triacylglycerols [342].

4.2.2 Imaging analysis of Compritol®888-based lipid nanoparticles

Light microscopy analysis suggested that immediately after production all Compritol®888-based SLN and NLC formulations contained no particles higher than 1 µm. Although this methodology is not suitable for determination of the mean particle size, the instrument is sensitive to detect larger particles in the micrometer range.
Concerning SEM analysis, representative scanning electron micrographs of Compritol®888-based SLN have been obtained and are shown in Fig. 4.20.

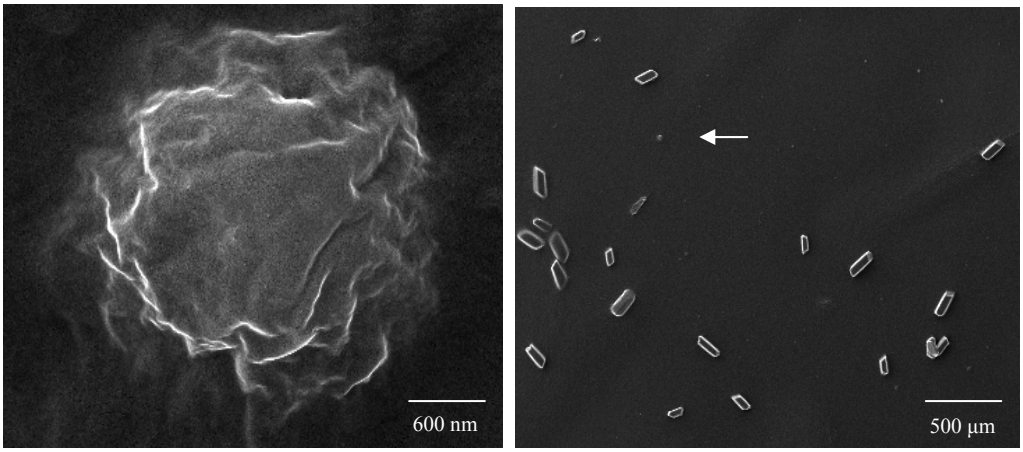

(a) SEM of SLN one week after production **(b)** SEM of SLN one year after production

Fig. 4.20: SEM pictures of Compritol®888-based lipid nanoparticles. (a) SLN with 3 µm, obtained one week after production; (b) SLN with 5 µm marked with arrow, obtained one year after production, where ketoconazole crystals can be seen.

One week after production Compritol®888-based SLN showed a relatively smooth but irregular surface, with a particle size of approximately 3 µm. Ketoconazole pictures show sedimentation of cylindrical-like drug crystals by SEM microscopy one year after production. This reveals that drug is outside the lipid nanoparticles.

4.2.3 Assessment of the physicochemical stability of ketoconazole

The chemical stability of pure ketoconazole has been evaluated by TGA (Fig. 4.21), previously to nanoparticle preparation by hot HPH. The analysis has been performed from

25ºC to 200ºC at a heating rate of 10 K/min, revealing no mass variation during the heating and cooling runs.

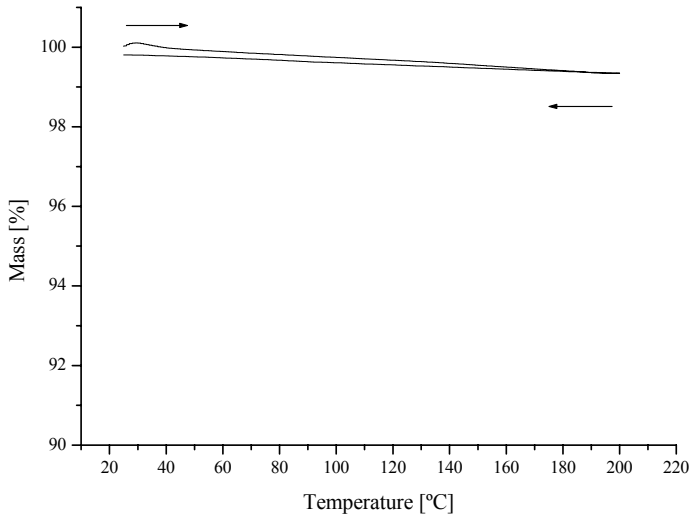

Fig. 4.21: TGA pattern of pure ketoconazole.

At temperatures above the recorded melting point of ketoconazole at approximately 151.22ºC (Fig 4.22, upper) the pure drug melted, showing no mass depending decomposition during the experiment. This result supports that ketoconazole should be chemically stable under the production conditions applied for preparation of these lipid carriers by HPH technique. Chemical degradation of ketoconazole is easy to detect by the change in colour to purple. In general, the human eye is highly sensitive to even slightly colour changes. Therefore, for this first basic study, to identify the most suitable formulation principle (SLN *vs* NLC), this criterion was sufficient. Directly after production, all aqueous SLN and NLC dispersions remained unchanged white. In case of homogenized dispersions being unstable, colour changes are detectable (e.g. omeprazole nanosuspensions [347]). From this, the result of white lipid suspensions is in agreement with the TGA data. During storage, light exposed ketoconazole-loaded SLN turned to purple indicating clearly the less suitability of this carrier system for ketoconazole. In this case, the alternative would be, of course, a light-excluding packaging.

The determination of the melting point of ketoconazole, as well as the enthalpy of the melting event has also been performed. This drug was analysed before and after tempering it for 1 hr at 90ºC (Fig. 4.22).

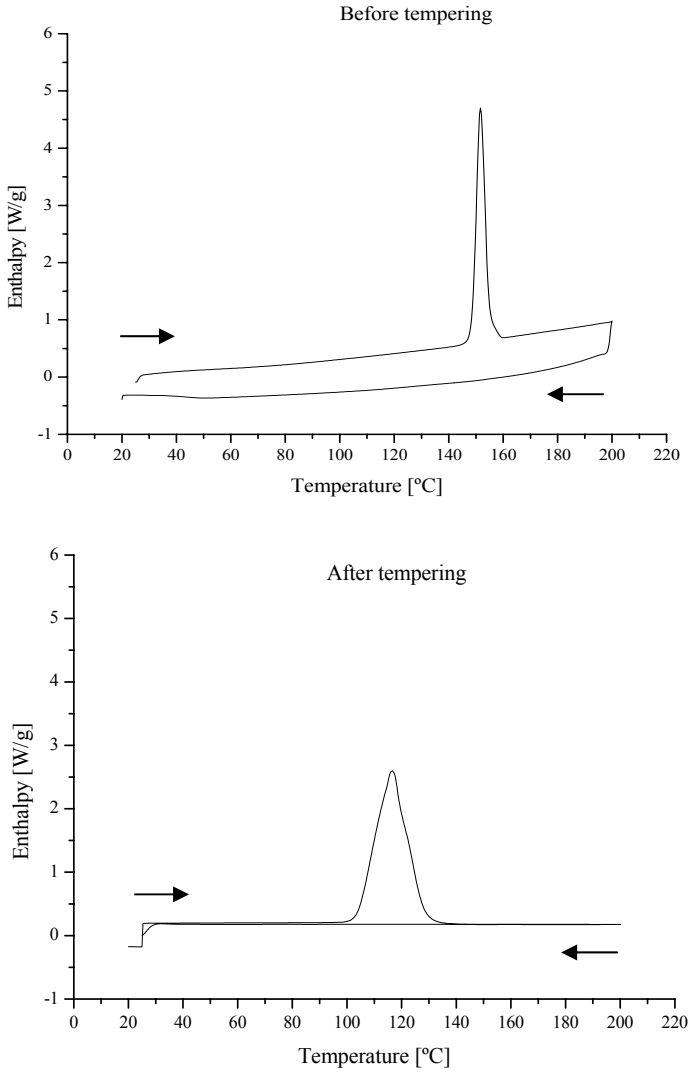

Fig. 4.22: DSC patterns of pure ketoconazole before (upper) and after (lower) tempering the drug under heat exposure (90ºC) for 1 hr.

Ketoconazole melted at 151.22ºC before tempering showing an enthalpy of 98.78 J/g (Fig. 4.22, upper). However, when the drug was heated for 1 hr at 90ºC a smaller and broader melting event has been observed at 116.67ºC (Fig. 4.22, lower) with a melting enthalpy of 98.13 J/g, which reveals that the drug is still crystalline, however it transforms to different polymorphic forms.

Polymorphic transformations of the drug have been confirmed by X-ray analysis. WAXS experiments have been performed before and after tempering the drug under heat exposure (90ºC) for 1 hr (Fig. 4.23). In the following WAXS curves the plots have been displaced vertically for better visualization.

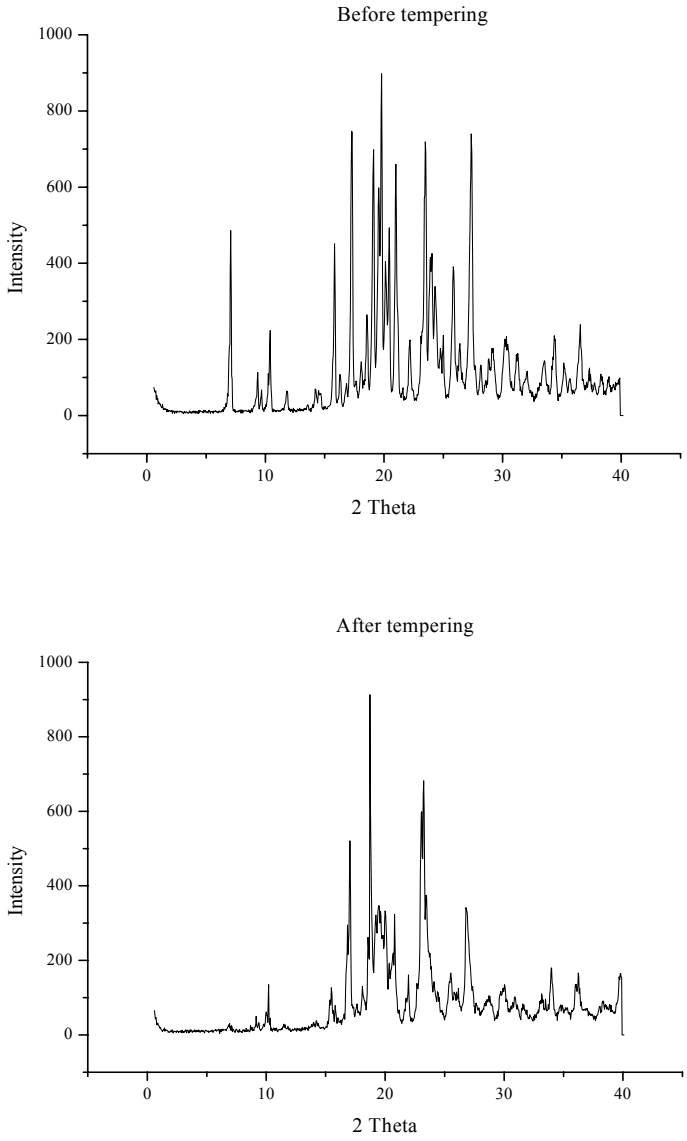

Fig. 4.23: X-ray diffraction patterns of pure ketoconazole recorded before (upper) and after (lower) tempering the drug under heat exposure (90ºC) for 1 hr.

Pure ketoconazole showed a crystalline state (Fig. 4.23, upper) before heat treatment. After tempering the diffractogram of the drug is totally different, revealing less peaks intensity as well as different polymorphic forms (Fig. 4.23, lower). These results show that ketoconazole is sensitive to thermal treatment and, therefore, for production of lipid nanoparticles by HPH technique, the process needs to be fast enough to avoid extensive thermal exposure of this drug.

4.2.4 Assessment of the polymorphic behaviour of lipid and drug

In order to elucidate the internal structure of Compritol®888-based SLN and NLC, a study on the recrystallization tendency of the lipid and the drug has been performed before and after the preparation of the systems.

4.2.4.1 Characterization of the bulk Compritol®888 ATO

For the characterization of the bulk Compritol®888, this lipid has been analysed by DSC before and after its tempering by incubation for 1 hr in an oven heated at 90ºC (Fig. 4.24). Table XIX shows the corresponding DSC data.

The first heating run (Fig. 4.24, upper) depicted a melting event at 71.73ºC and a very small endothermic peak at approximately 51.20ºC. Once this lipid is not composed of pure triacylglycerols, but mono-, di- and triacylglycerols of behenic acid (C_{22}), the observed melting peak might be due to a mixture of metastable polymorphic forms. The peak at lower temperature corresponds to the melting of the α modification, which in Compritol®888 it is very unstable and disappears after a second thermal stress (Fig. 4.24, middle). The onset temperature of the first curve has been recorded at 61.25ºC, whereas the second curve showed an onset temperature of 59.35ºC. The decrease of the onset temperature broaden the melting peak, which impair the increase in the β'/β_i amounts in the lattice of the bulk lipid after thermal stress. Comparing the first and the second curves, the decrease of the melting enthalpy values was from 138.03 J/g to 114.72 J/g, showing a small difference between both DSC patterns.

Concerning the recrystallization temperatures (corresponding to the cooling runs) similar exotherms have been obtained. The first and second exotherms patterns of Fig. 4.24 are very similar, showing a very small protuberance that might correspond to the α modification (arrow), which once again slightly disappears after tempering (Fig. 4.24, lower).

With regard to the first heating run after tempering (Fig. 4.24, lower), a higher melting point was recorded (72.4ºC) with a melting enthalpy of 122.19 J/g and the fraction corresponding to the α modification of the lipid is practically absent. Also major differences were observed in the cooling fraction of this curve. In fact, a less pronounced polymorphic form (smaller shoulder) of Compritol®888 was registered. After tempering, the input of energy is sufficiently high that the lipid changes from a more unstable to a more stable polymorphic form. Therefore, it can be emphasized that after tempering the lipid is a mixture of isomers.

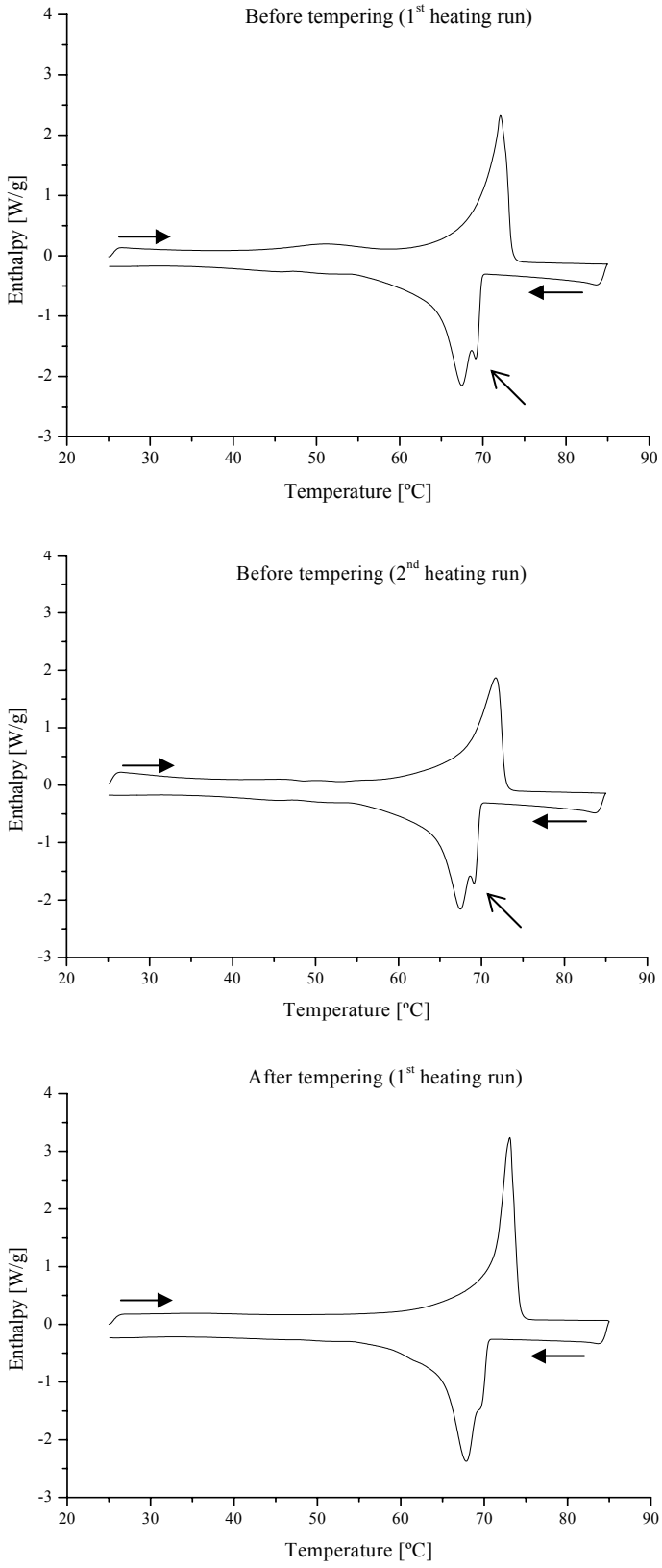

Fig. 4.24: DSC patterns of bulk Compritol®888 ATO recorded before (upper and middle) and after (lower) tempering the lipid under heat exposure (90ºC) for 1 hr.

Table XIX: DSC parameters of bulk Compritol®888 ATO recorded before and after tempering the lipid under heat exposure (90ºC) for 1 hr.

Curves of bulk Compritol®888 ATO	Melting point (ºC)	Onset (ºC)	Integral (mJ)	Enthalpy (J/g)
First heating run before tempering	71.73	61.25	625.14	138.03
Second heating run before tempering	71.47	59.35	519.55	114.72
First heating run after tempering	72.44	62.71	728.04	122.19

Polymorphic behaviour is often shown by long-chain compounds such as previously observed for Dynasan®116 [299]. In general, those compounds crystallize in two or three different phases, α and β', or α, β' and β, respectively [348]. Usually DSC is used to investigate these different lipid phases in a daily basis, but X-ray diffraction is much more suitable technique for identification since each polymorph has its own distinctive diffraction pattern.

Regarding the WAXS analysis, the studies of the lamellae arrangement of Compritol®888 molecules have also been performed without pre-treatment (Fig. 4.25, upper) and after tempering the lipid at 90ºC for 1 hr (Fig. 4.25, lower).

Significant differences have been observed between both diffractograms. Before tempering, the lipid shows two major reflections, one at 21.04 (2θ), i.e. d = 0.43 nm, and another at 23.36 (2θ), i.e. d = 0.38 nm. These two signals correspond to the β' modifications typical from triacylglycerols [326]. After tempering, the intensity of the peaks decreased significantly, revealing now only one peak at 21.04 (2θ), i.e. d = 0.43 nm, having a small shoulder at 23.40 (2θ), i.e. d = 0.39, also corresponding to the β' modifications. The only difference between both curves is the intensity and the width of the peak (resolution of two peaks), which depends on different factors such as the amount of sample mounted on the glass capillary and particle size. However, it is clear that the lipid slightly changes its crystallinity by tempering as observed by DSC analysis.

It is known that the phase transformations of triacylglycerols and their mixtures are monotropic (α → β', α → β' → β, or α → β) [254], implicating only one stable polymorphic form. For monoacid even-numbered triacylglycerols $C_nC_nC_n$ the most stable modification is β, whereas for the $C_nC_{n+2}C_n$ and $C_nC_{n+4}C_n$ the most stable polymorphic form is β'. For mixtures of mono-, di- and triacylglycerols such as Compritol®888, a difference in relative phase stability exists as well. From the obtained X-ray pattern before tempering (Fig. 4.25, upper) one can realize that this lipid shows a shift reflection between 19º < 2θ < 22º of high intensity and between 22º < 2θ < 24º of low intensity. After tempering, those two peaks were no more

recorded, meaning that for this lipid the most stable polymorphic form is β' (Fig. 4.25, lower, arrow). These results are in agreement with the ones obtained with DSC once the recorded melting point after tempering was slightly higher than before tempering (0.7ºC), however depicting lower melting enthalpy (122.19 J/g in comparison to 138.03 J/g).

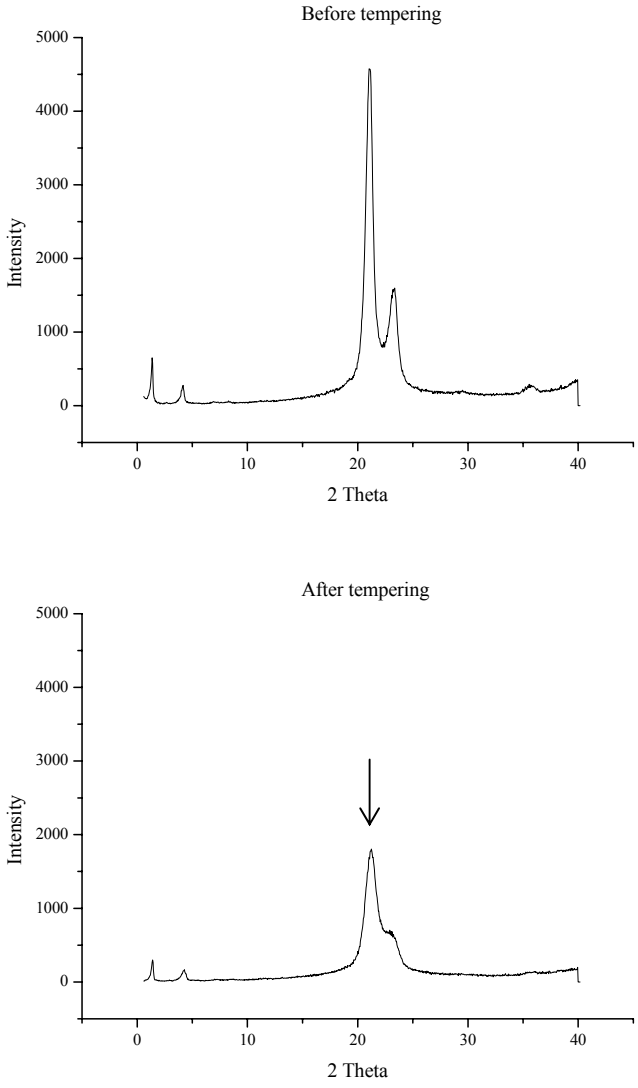

Fig. 4.25: X-ray diffraction patterns of bulk Compritol®888 ATO recorded before (upper) and after (lower) tempering the lipid under heat exposure (90ºC) for 1 hr.

4.2.4.2 Characterization of the physical mixtures of bulk lipid and drug

The physical mixture of bulk Compritol®888 ATO with 0.75% (m/m) of ketoconazole has also been analysed by DSC and by X-ray diffraction for the assessment of polymorphic modifications of the lipid in the presence of ketoconazole.

4.2.4.2.1 DSC analysis

DSC analysis has been performed before and after tempering the mixture under heat exposure (90ºC) for 1 hr (Fig. 4.26). Table XX shows the registered DSC parameters.

Once ketoconazole has a crystalline character a melting event should have been detected in the DSC runs of physical mixtures of drug and lipid if the former was not soluble. The results revealed only the melting events of the lipid at 72.66ºC (enthalpy of 133.55 J/g) showing that the drug is molecularly dispersed in the lipid, dissolved in the lipid phase during melting of the lipid when heating the mixture (Fig. 4.26, upper). As depicted in Table XX, after tempering the mixture the melting point slightly decreased to 72.08ºC, with an enthalpy of 119.09 J/g (Fig. 4.26, lower). The unresolved melting peak (72.66ºC) obtained before tempering (Fig. 4.26, upper) shows the presence of "impurity" in the bulk lipid, i.e. the presence of ketoconazole, because a depression in the melting peak of Compritol®888 occurs (enthalpy of bulk is 138.03 J/g, Table XIX). This unresolved peak disappears after tempering (Fig. 4.26, lower). The obtained patterns support the conclusion that ketoconazole does not have a crystalline character in this mixture.

In order to evaluate the distortions of the crystal lattice of Compritol®888 matrix by the addition of α-tocopherol, the physical mixtures of solid lipid, liquid lipid and drug were analysed by DSC as well (Fig. 4.27, Table XXI). An increase in crystal order disturbance (lattice defects) led to a reduction of the onset temperature and of the melting peak. Before tempering the mixture, the presence of the stable β polymorph was hardly detected, while after tempering the presence of β form was recorded at approximately 66.20ºC. Before tempering, the heating curve revealed a less pronounced shoulder (Fig. 4.27, upper), which corresponds to the presence of "impurities" in the bulk lipid (Fig. 4.24, upper). After tempering no more shoulder is visible being substituted by a broad peak with an onset temperature of 63.14ºC (Fig. 4.27, lower).

Comparing with the results obtained for bulk lipid (Table XIX), the melting enthalpy decreased significantly, from 138.03 J/g to 94.54 J/g (Table XXI).

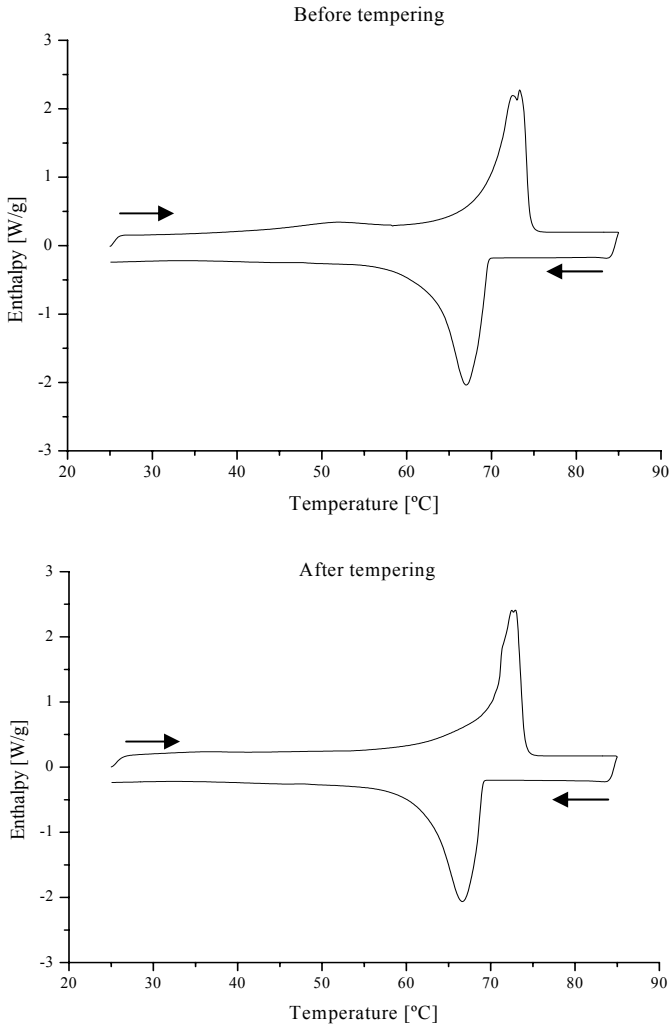

Fig. 4.26: DSC patterns of physical mixtures of Compritol®888 ATO and ketoconazole (99+1) recorded before (upper) and after (lower) tempering the mixture under heat exposure (90ºC) for 1 hr.

Table XX: DSC parameters of physical mixtures of Compritol®888 ATO and ketoconazole (99+1) recorded before and after tempering the mixture under heat exposure (90ºC) for 1 hr.

Curves of physical mixtures of Compritol®888 and ketoconazole	Melting point (ºC)	Onset (ºC)	Integral (mJ)	Enthalpy (J/g)
Before tempering	72.66	61.94	1184.73	133.55
After tempering	72.08	59.80	1241.84	119.09

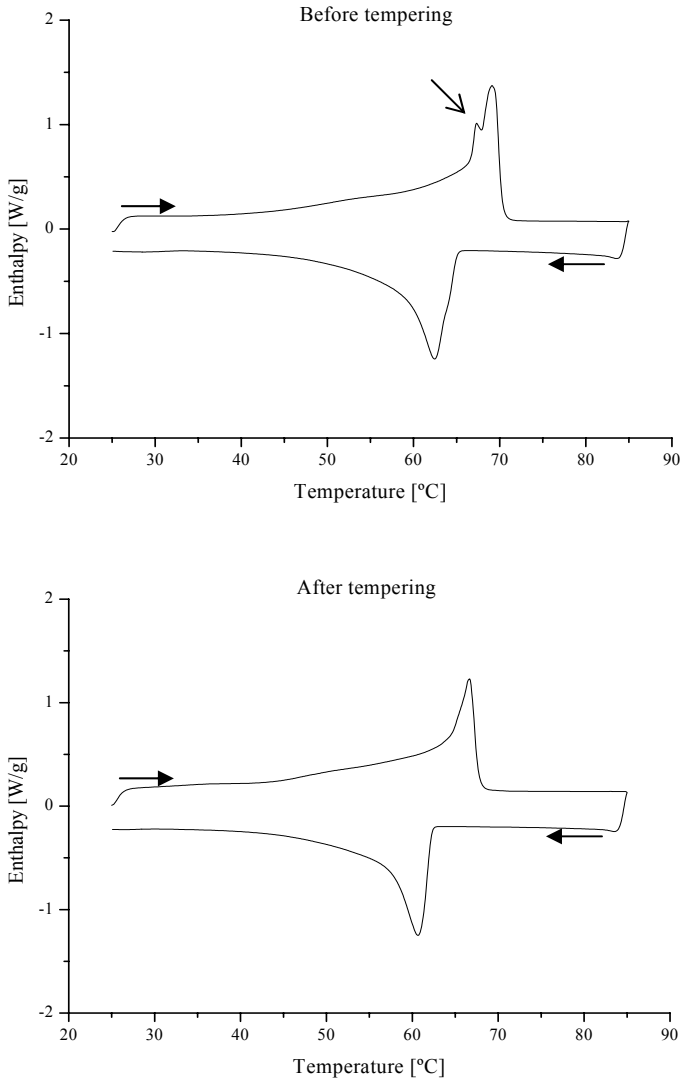

Fig. 4.27: DSC patterns of physical mixtures of Compritol®888 ATO, α-tocopherol and ketoconazole (69.3+29.7+1) recorded before (upper) and after (lower) tempering the mixture under heat exposure (90ºC) for 1 hr.

Table XXI: DSC parameters of physical mixtures of Compritol®888 ATO, α-tocopherol and ketoconazole (69.3+29.7+1) recorded before and after tempering the mixture under heat exposure (90ºC) for 1 hr.

Curves of mixtures of Compritol®888, α-tocopherol and ketoconazole	Melting point (ºC)	Onset (ºC)	Integral (mJ)	Enthalpy (J/g)
Before tempering	68.72	66.19	757.94	94.54
After tempering	66.20	63.14	892.07	77.00

The presence of α-tocopherol was also observed during the cooling process in both curves. Concerning the recrystallization process, the broadened exotherms recorded between 63ºC and 61ºC both before and after tempering shows the presence of the liquid oil. The difference of shape between them is due to the presence of well defined polymorphic modifications.

4.2.4.2.2 X-ray diffraction analysis

Concerning the X-ray analysis, significant differences of the lamellae arrangements of the fatty acid chains of Compritol®888 with ketoconazole have also been registered (Fig. 4.28), as previously observed for the bulk lipid (Fig. 4.25). Before tempering, the mixture shows two main typical signals of triacylglycerols (Fig. 4.28, upper) occurring at 21.08 (2θ) and at 23.36 (2θ), i.e. at 0.43 nm and 0.38 nm, respectively. These signals correspond to the metastable β' modification [323, 324], revealing that the mixture has an orthorhombic sub-cell packing [326]. A very small protuberance at 19.24 (2θ), i.e. d = 0.46 nm occurs previously to tempering the mixtures. This signal corresponds to the most stable polymorphic form β of triacylglycerols, which disappears after tempering. After tempering only one peak at 21.08 (2θ) having a shoulder at 23.04 (2θ) was recorded (Fig. 4.28, lower). These signals are the same as the ones recorded before tempering, however of lower intensity.

Comparing both Figs. 4.25 and 4.28, similar patterns have been obtained which emphasizes the fact that ketoconazole does not influence the crystal lattice of bulk Compritol®888. The main changes occur in the lipid during thermal treatment.

The physical mixtures of Compritol®888, α-tocopherol and ketoconazole also showed different X-ray patterns before and after heat exposure (Fig. 4.29). Tempering the mixture of the three components changed the crystallinity of the side chains proven by the detection of different patterns with a broadened peak.

The typical signal of β modification recorded before tempering the mixture of lipid and drug (Fig. 4.28, upper) were also obtained in the mixture of the three components (Fig. 4.29, upper), and did not disappear after tempering, i.e. the signal at 19.24 (2θ), i.e. d = 0.46 nm (Fig. 4.29, lower). The same peaks characteristics of the most stable polymorphic form β of triacylglycerols, also occurred however of lower intensity after tempering the mixture.

Another important observation is the analysis of the baseline of both curves. The addition of the oil α-tocopherol to the mixture of solid lipid and drug increased the lattice disturbance of this latter, which is easily detected comparing the baselines of the patterns of Fig. 4.28 and 4.29. Whereas the pure Compritol®888 exhibited the β' form, the addition of α-tocopherol led

to a bulk material probably consisting of β' and smaller amounts of β_i. It is well known that the introduction of short or medium chain components generally accelerates the rate of polymorphic transitions, which can be observed here as well.

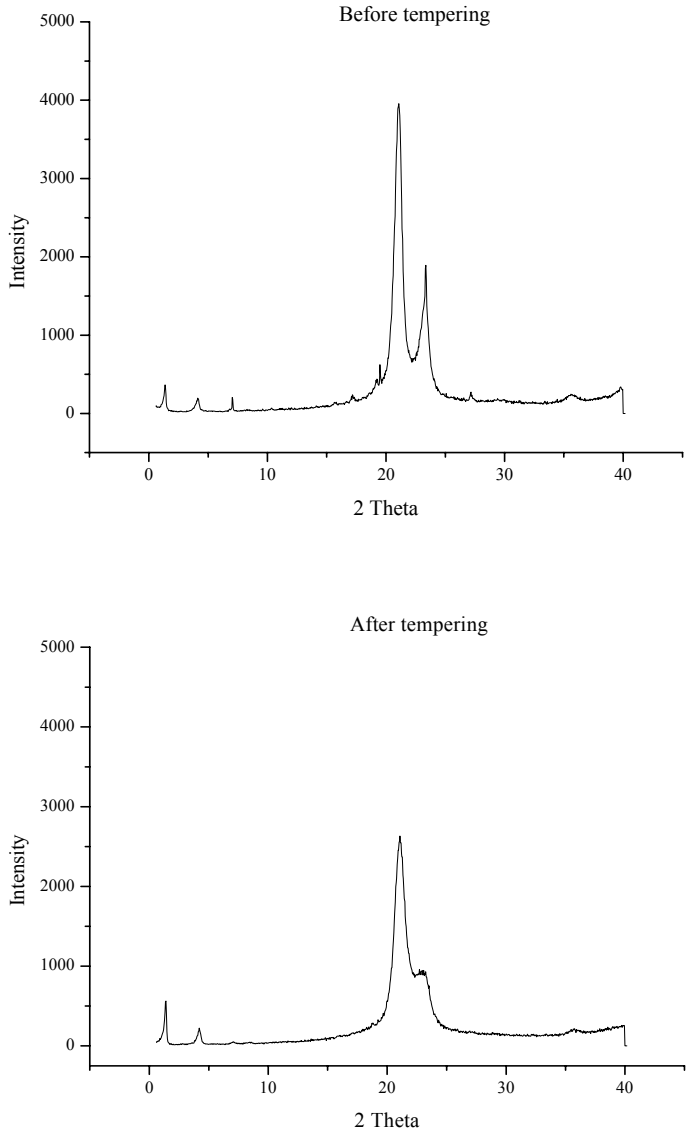

Fig. 4.28: X-ray diffraction patterns of physical mixtures of Compritol®888 ATO and ketoconazole (99+1) recorded before (upper) and after (lower) tempering the mixture under heat exposure (90ºC) for 1 hr.

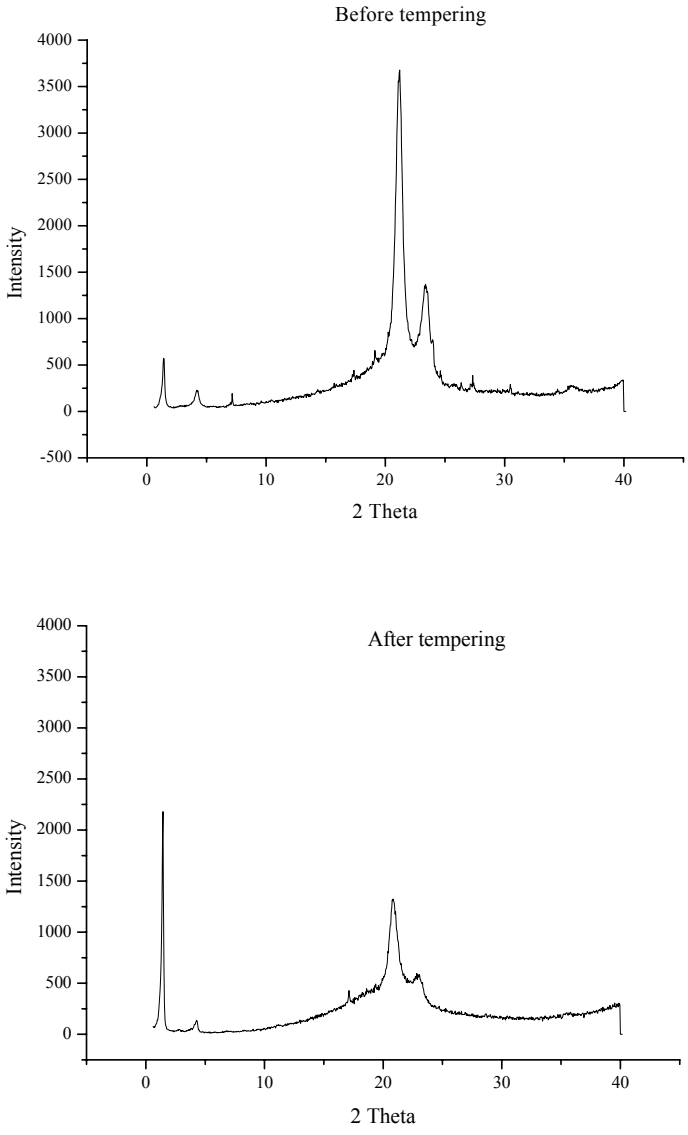

Fig. 4.29: X-ray diffraction patterns of physical mixtures of Compritol®888 ATO, α-tocopherol and ketoconazole (69.3+29.7+1) recorded before (upper) and after (lower) tempering the mixture under heat exposure (90ºC) for 1 hr.

4.2.4.3 Characterization of the Compritol®888-based SLN and NLC

4.2.4.3.1 DSC analysis

Tables XXII and XXIII show the melting and the crystallization parameters of Compritol®888-based nanoparticles, respectively, obtained by DSC analysis after three months and one year of storage at 4ºC and at 25ºC.

Table XXII: DSC parameters of aqueous Compritol®888-based SLN dispersions recorded after three months (M3) and one (Y1) year of storage at two different temperatures. (25ºC^{dark} stands for samples containing ketoconazole stored at 25ºC under light protection).

DSC parameters		C888SLN		C888SLN_Ke		
		4ºC	25ºC	4ºC	25ºC	25ºC^{dark}
mp (ºC)	M3	70.65	73.17	70.52	70.64	71.04
	Y1	72.34	74.09	71.94	71.83	72.49
Onset (ºC)	M3	68.45	71.11	67.96	68.06	68.63
	Y1	70.27	72.09	69.13	70.32	70.92
Integral (mJ)	M3	455.27	339.91	614.31	424.97	510.68
	Y1	476.89	409.36	627.22	494.13	526.61
Enthalpy (J/g)	M3	17.75	12.97	15.69	16.21	16.23
	Y1	20.89	15.21	18.94	19.34	19.49
RI (%)	M3	85.6	62.5	75.6	78.1	78.2
	Y1	100.0	73.5	91.5	93.4	94.1

DSC allowed determination of thermotropic phase transitions in a quantitative manner and it is especially useful for the investigation of the complex behaviour of polymorphic triacylglycerols once dispersed in an aqueous phase [256]. The recorded melting point of Compritol®888-based nanoparticles slightly decreased in comparison to the one obtained for bulk lipid, i.e. melting point of Compritol®888 was 71.73ºC (Table XIX). However, it increased during storage time (Table XXII). The difference between the registered onset and melting point values can be taken as a measure for the width of melting peaks of each formulation. The thermal curves of lipid nanoparticles recorded during DSC analysis displayed pronounced melting peaks.

The RI values obtained for NLC formulations were lower than for SLN formulations with the same lipid content. The presence of drug decreased the crystallinity of the lipid nanoparticles. The effect of temperature of storage in the RI values was more pronounced for drug-free samples. After one year, SLN showed higher RI at 4ºC whereas NLC revealed higher values when stored at 25ºC. For drug-loaded samples the differences observed between the storage temperatures were not of relevance. In general, crystal ordering of NLC decreases in comparison to the recorded DSC run for SLN with the same lipid content. This is in agreement with the theory that NLC are characterized by a less ordered, less crystalline structure as their special feature [349].

Table XXIII: DSC parameters of aqueous Compritol®888-based NLC dispersions recorded after three months (M3) and one (Y1) year of storage at two different temperatures. (25ºC^{dark} stands for samples containing ketoconazole stored at 25ºC under light protection).

DSC parameters		C888NLC		C888NLC_Ke		
		4ºC	25ºC	4ºC	25ºC	25ºC^{dark}
mp (ºC)	M3	67.05	65.39	69.11	66.99	66.13
	Y1	69.27	68.76	71.23	68.94	67.89
Onset (ºC)	M3	55.44	38.29	62.77	56.36	55.37
	Y1	57.37	51.22	64.43	59.57	57.49
Integral (mJ)	M3	307.86	342.33	189.06	356.86	308.67
	Y1	324.34	369.41	302.11	413.52	332.81
Enthalpy (J/g)	M3	12.35	16.86	12.59	14.02	10.49
	Y1	14.42	19.23	15.24	16.47	12.97
RI (%)	M3	59.5	81.3	60.7	67.6	50.6
	Y1	69.6	92.9	73.6	79.6	62.6

Ketoconazole-loaded SLN yield a narrower peak than ketoconazole-loaded NLC, which shows a very broad transition stretching. As the fatty acid profiles of both are comparable, this difference must be a result of the higher content of minor components present in the NLC formulation (i.e. the oil molecules). The difference in the DSC thermograms observed here was attributed to the presence of α-tocopherol in the NLC formulation, which may well account for the measurable lowering of the transition enthalpy. The oil distorts the crystal formation, as intended in the NLC concept. No peaks arising from ketoconazole could be observed, revealing that the drug is soluble in the lipid matrix of both formulations.

4.2.4.3.2 X-ray diffraction analysis

WAXS experiments were performed to assess the influence of the drug and the oily component on the subcell parameters and long spacings of the solid Compritol®888 nanoparticles and to confirm polymorphism established by the DSC results. Fig. 4.30 shows the X-ray diffraction patterns of aqueous Compritol®888-based SLN and NLC dispersions recorded after three months of storage at room temperature. The results obtained after one year at 25ºC under light protection are shown in Fig. 4.31 for ketoconazole-loaded SLN and NLC.

The drug-free Compritol®888-based SLN (Fig. 4.30, upper left) revealed a diffraction pattern very similar to that of bulk lipid thus being in the β' state (Fig. 4.25, upper). A small third peak at 0.46 nm arose with the incorporation of the oil (arrow), i.e. for the preparation of NLC is the indication of partial formation of β_i (Fig. 4.30, upper right). It seems not possible to clearly identify β' or β_i or mixtures thereof by their short spacings shown in these patterns. Usually different polymorphs display different long spacings as well. A mixture of two polymorphs leads to two distinguishable long spacings. Therefore, it should be possible to differentiate between β' and β_i and mixtures by their long spacings. However, in this special case of β' and β_i no such differences in long spacing can be detected and thus no further information on this special polymorphism can be derived. Even without clear nomenclature, one can conclude that the oil has a measurable impact on the crystal ordering by favouring the formation of an intermediate β form.

From Fig. 4.30 it is not conceivable that the oil used to prepare NLC formulations is totally inserted between the bilayers planes of the Compritol®888 crystals after three months of storage at room temperature, even under dark conditions. The incorporation of the oil in Compritol®888-based nanoparticles might change the chain length structure, which is a repetitive sequence of acyl chains involved in a unit lamellae along the chain axis, from double to triple [350]. These alterations in structure would lead to changes in the long spacings in magnitude of at least 0.5 to 1 nm. Regarding the influence of storage condition, i.e. under light protection, no major differences have been recorded either for SLN or for NLC formulations containing ketoconazole.

The bulk material (Fig. 4.25), as well as drug-loaded and drug-free SLN formulations (Fig. 4.30, left patterns), revealed diffraction patterns very similar, showing the typical signals of the triacylglycerols after three months of storage at room temperature [323, 324], whereas

NLC formulations showed a small third peak at 0.46 nm indicating the partial formation of an intermediate β_i form [341] (Fig. 4.30, right patterns).

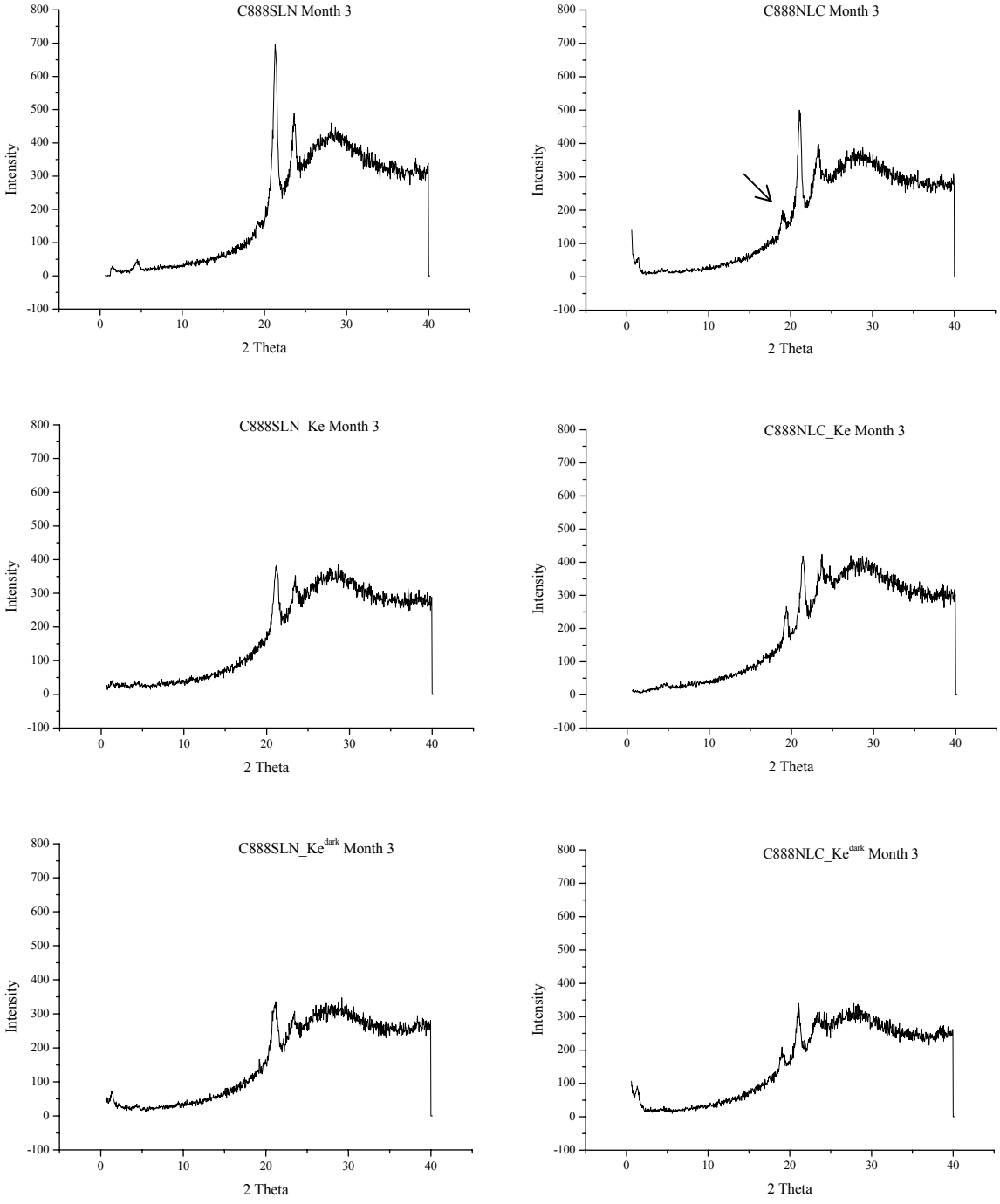

Fig. 4.30: X-ray diffraction patterns of aqueous Compritol®888-based SLN and NLC dispersions recorded after 3 months of storage at room temperature. (25ºC^{dark} stands for samples containing ketoconazole stored at 25ºC under light protection).

X-ray diffraction investigations have been most valuable in the elucidation of the manner of arrangement of lipid molecules, their multiple-melting phenomena, phase behaviour and the characterization and identification of the structure of lipid and drug molecules [303].

Lower transition temperatures observed by DSC for NLC formulations were confirmed by X-ray diffraction analysis. In fact, the broader peaks obtained for these formulations result from less crystal order and increased number of crystal defects. After one year the SLN samples show the well known scattering peaks of Compritol®888, indicating that the lipid matrix of such carriers has some crystalline character (Fig. 4.31, left).

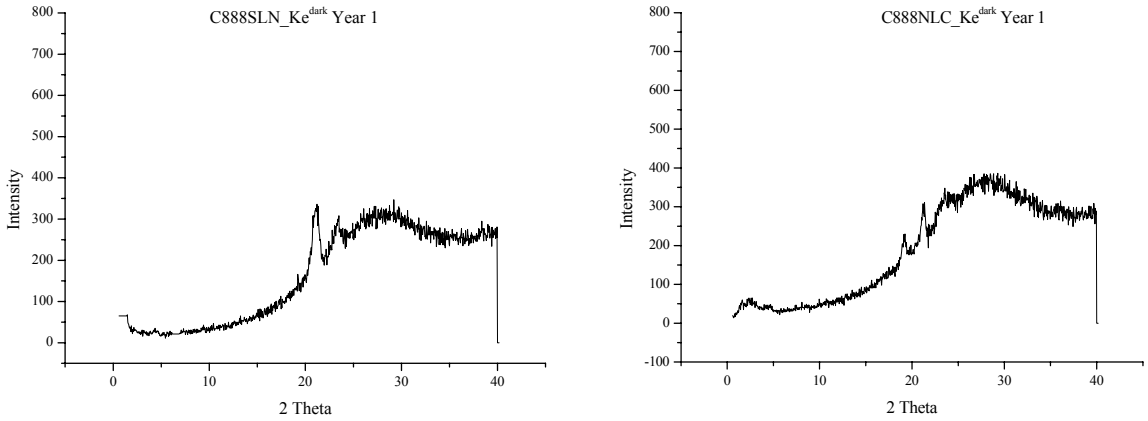

Fig. 4.31: X-ray diffraction patterns of aqueous Compritol®888-based SLN and NLC dispersions recorded after 1 year of storage at room temperature under light protection.

Interesting was the presence of peaks after running NLC samples indicating the presence of a crystalline structure (Fig. 4.31, right). These results might impair the expulsion of some of the oil from the Compritol®888 matrix during shelf life. In both types of carriers the presence of drug influenced the rearrangement of fatty acid chains in the lipid matrix, decreasing their crystallinity. These data support the incorporation of some of the ketoconazole in molecularly dispersed form in between the fatty acid chains of the highly mobile liquid crystalline α modification of the loaded SLN and NLC. However, in agreement with the observed by SEM analysis (Fig. 4.20), some of the drug is expelled during storage time due to the polymorphic transformations that increased the crystallinity of the lipid nanoparticles.

4.2.5 Assessment of the chemical stability of ketoconazole in SLN and NLC

The presence of visible particles and/or ketoconazole crystals in the developed formulations provides an indication of their physicochemical stability. In this case, Compritol®888-based SLN and NLC have been optimized in terms of physicochemical stability and the incorporation of ketoconazole decreased the stability of the aqueous dispersions.

The chemical stability of ketoconazole has been therefore assessed by HPLC analysis, in comparison to a reference emulsion prepared using α-tocopherol as internal phase stabilized with a surfactant/co-surfactant system in the same concentration (2.5% m/m Poloxamer®188 and 0.125% m/m sodium deoxycholate), as the one used for the production of lipid nanoparticles. Fig. 4.32 depicts the percentage of ketoconazole recovered from C888SLN_Ke and from C888NLC_Ke, in comparison to the reference emulsion (RefEm_Ke), during two years of storage at different storage conditions. Those values have been determined against an appropriate calibration curve (Fig. 3.11, Chapter 3) obtained using acetone as organic solvent for the formulations.

Immediately after production the percentage of drug recovered was 62.1% for C888SLN_Ke and 70.3% for C888NLC_Ke. During shelf life, a decrease of the amount of drug recovered has been observed after two years, i.e. 13.9% for C888SLN_Ke and 20.7% for C888NLC_Ke, once stored at 25ºC. After two years of storage at the same temperature 2.7% of drug has been recovered from the prepared reference emulsion. This reference emulsion showed a similar mean particles size obtained by PCS, approximately 189 nm with a PI of 0.223, thus those results could be compared. The storage at 4ºC slightly increased the percentages of drug recovered from the systems, i.e. to 15.6%, 41.9% and 51.4% for RefEmul_Ke, C888SLN_Ke and C888NLC_Ke, respectively.

Despite of the advantages of complex acylglycerols such as higher drug loading, surfactant activity and less ordered crystal packing, preparation of SLN for entrapment of a labile drug such as ketoconazole was not successful. However, in comparison to the reference emulsion SLN could better stabilize this drug. More promising were NLC formulations especially under dark storage conditions. Form Fig. 4.32 it is perfectly clear that α-tocopherol protected ketoconazole from light exposure damage. This antioxidant was able to significantly decrease the amount of drug under degradation. Possible mechanisms of antioxidant activity described in the literature are transition metal chelation, direct radical scavenging and reduction by electron donation [351].

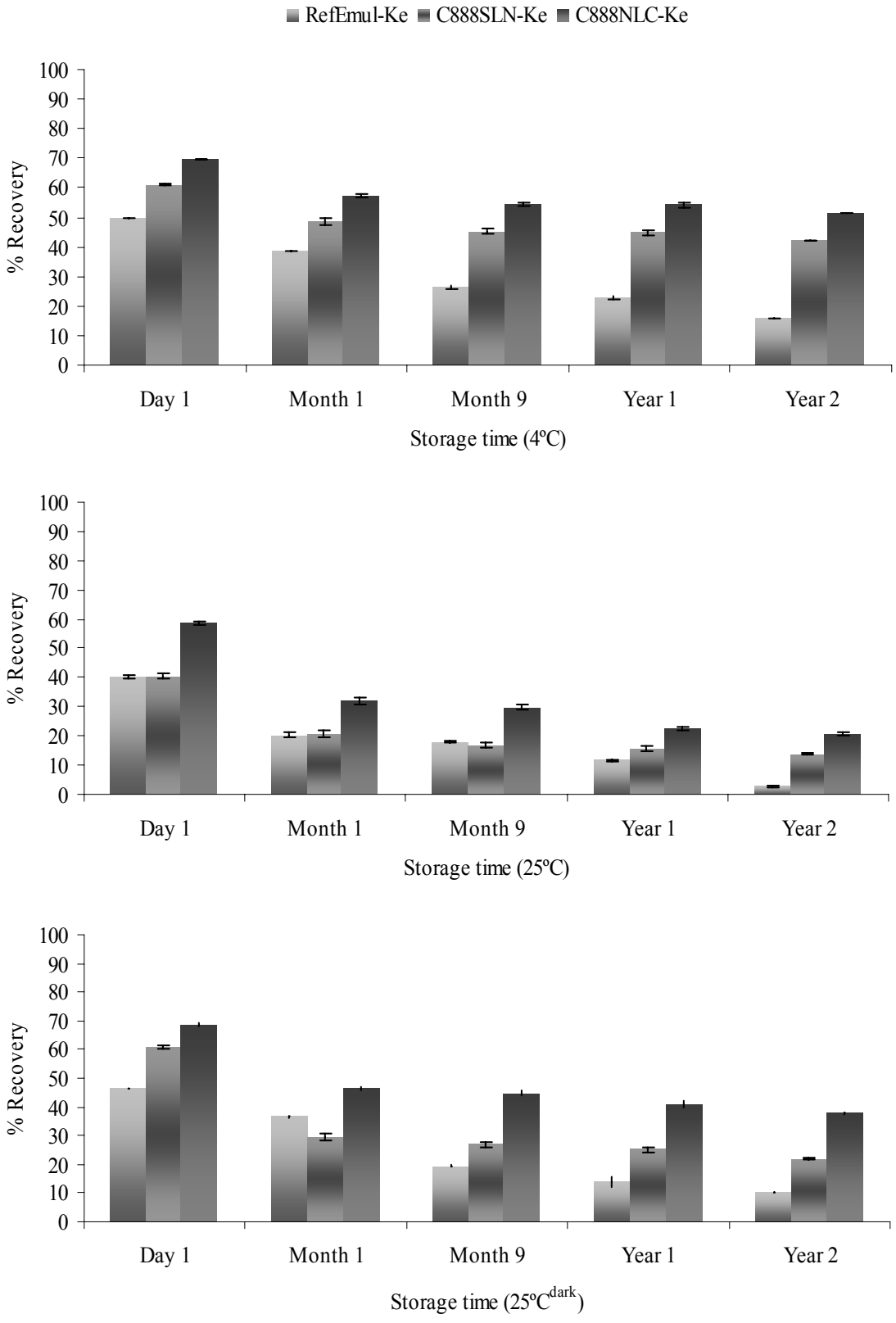

Fig. 4.32: Percentage of drug recovered during two years of storage at 4ºC, 25ºC, 25ºC^{dark} for C888SLN-Ke and C888SLN-Ke in comparison to a reference emulsion.

4.2.6 Rheological analysis of Compritol®888-based lipid nanoparticles

A strain sweep test has been performed for all different Compritol®888-based lipid nanoparticles previously to oscillatory testing, in order to determine the linear viscoelastic region, which revealed to be 1 Pa. Therefore, in this section all measurements were carried out at a stress amplitude of 1 Pa.

4.2.6.1 Immediately after production

On the day of production of Compritol®888-based lipid nanoparticles, the drug-free and drug-loaded SLN and NLC have been analysed applying a frequency from 0.1 to 10 Hz (Figs. 4.33 and 4.34).

Concerning the aqueous SLN dispersions, no major differences have been observed between ketoconazole-free (Fig. 4.33, upper) and ketoconazole-loaded (Fig. 4.33, lower) formulations. For both systems all viscoelastic parameters (G', G" and complex viscosity) were highly dependent on the applied frequency, meaning that these systems have a weak structure.

In the oscillation frequency sweep test applied to C888SLN the values of the storage modulus (G', elastic component) did not differ significantly from those recorded for the loss modulus (G", viscous component). Although during the assay the tan δ remained lower than 1, at a frequency of 7 Hz the tan δ was recorded to be approximately 8, being again lower than 1 at 10 Hz. This inflection of the recorded results shows the weak structure of these formulations. Therefore, it cannot be associated to a perfect elastic-like behaviour.

When incorporating ketoconazole (C888SLN_Ke) the elastic component G' increased significantly with increasing the applied frequency. This behaviour shows the ability to resist to structural changes under stress [352]. Under the increasing frequency, G' was clearly higher than G" showing a more elastic-like behaviour. However, the increase in complex viscosity with the increase of the applied frequency also shows a different behaviour from the typical pseudoplastic materials.

With regard to the aqueous NLC dispersions, the major differences have been obtained for G' and for the complex viscosity values between ketoconazole-free (Fig. 4.34, upper) and ketoconazole-loaded (Fig. 4.34, lower) formulations. C888NLC revealed a more elastic than viscous behaviour once G' was much higher than G". In addition, for this formulation the viscosity decreased with the increase of the applied frequency, which indicates a pseudoplastic behaviour. After incorporation of drug, a more weak system was obtained due

to the higher dependency of the all viscoelastic parameters on the applied frequency. Moreover, lower magnitude values have been recorded for all viscoelastic parameters, in comparison to the C888NLC.

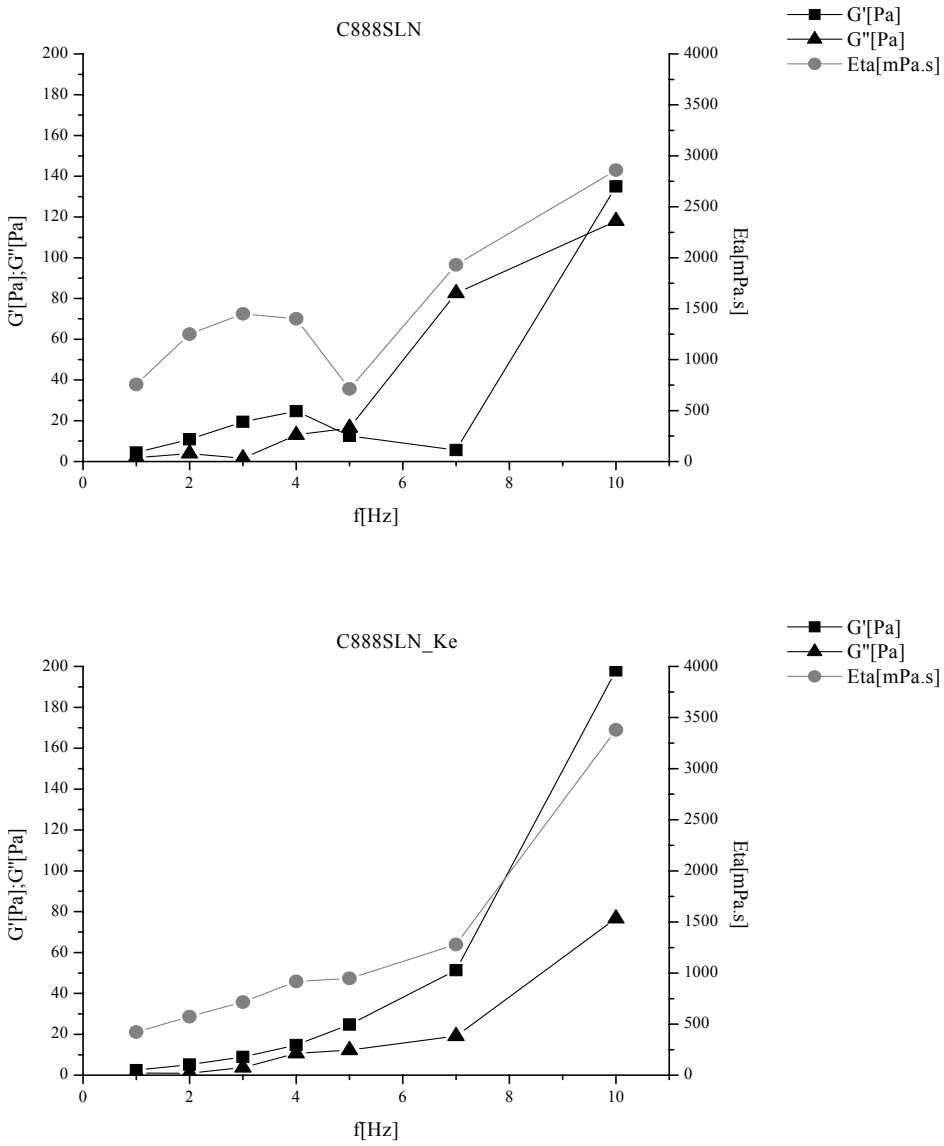

Fig. 4.33: Storage modulus (G'), loss modulus (G'') and complex viscosity (Eta) of aqueous Compritol®888-based SLN dispersions as a function of frequency, recorded immediately after production under a constant stress amplitude of 1 Pa.

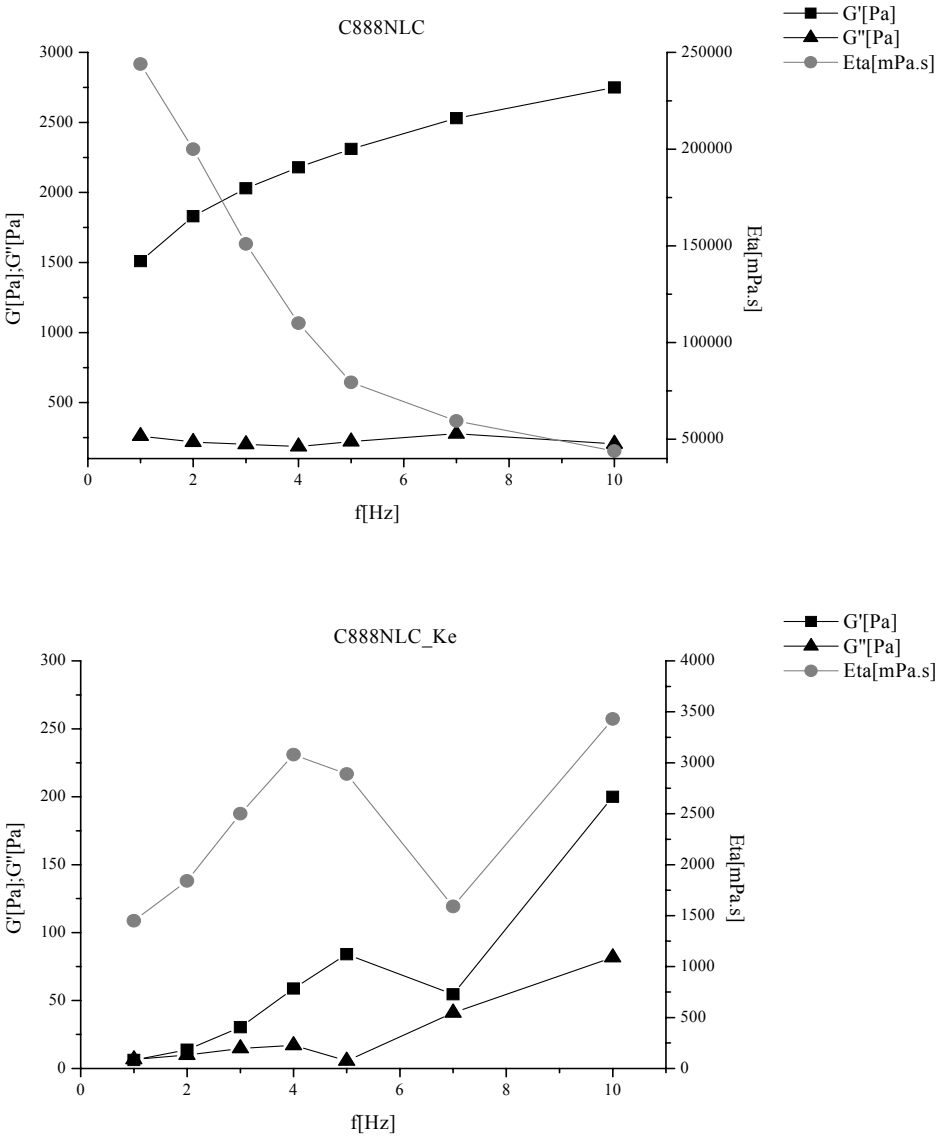

Fig. 4.34: Storage modulus (G'), loss modulus (G'') and complex viscosity (Eta) of aqueous Compritol®888-based NLC dispersions as a function of frequency, recorded immediately after production under a constant stress amplitude of 1 Pa.

4.2.6.2 At different temperatures of storage

Viscoelastic parameters have been evaluated after one month of storage at different conditions, under a constant stress amplitude of 1 Pa. Table XXIV depicts the obtained results.

Table XXIV: Storage modulus (G'), loss modulus (G'') and complex viscosity (Eta) of aqueous Compritol®888-based SLN and NLC dispersions as a function of frequency, recorded after one month of storage at two different temperatures, under a constant stress amplitude of 1 Pa. (25ºC^{dark} stands for samples containing ketoconazole stored at 25ºC under light protection).

Sample	Storage temperature	f [Hz]	G' [Pa]	G'' [Pa]	Eta [mPa.s]
C888SLN	4ºC	1	5	3	936
		10	142	16	2270
	25ºC	1	6	4	1150
		10	140	142	3170
C888SLN_Ke	4ºC	1	4	2	753
		10	189	27	3050
	25ºC	1	4	2	749
		10	284	18	4530
	25ºC^{dark}	1	6	3	1020
		10	192	61	3210
C888NLC	4ºC	1	954	165	154000
		10	1620	272	26100
	25ºC	1	1210	137	19300
		10	1450	257	23500
C888NLC_Ke	4ºC	1	8	8	1850
		10	272	54	4410
	25ºC	1	14	12	2950
		10	347	147	6000
	25ºC^{dark}	1	3	2	525
		10	188	0	3000

In all storage conditions, all formulations showed that G', G" and complex viscosity are highly dependent upon the applied frequency, i.e. they increase with the increase of the frequency. An exception of this pattern has been detected for the values of G" for C888NLC_Ke stored at room temperature under dark conditions. The recorded values are, however, very low.
Although being relatively weak structures, these systems revealed a more elastic behaviour once G' (elastic component) showed to be higher than G" (viscous component). Storage of the systems at 4ºC could be a promising alternative to avoid weaken of the structure.

4.2.6.3 During shelf life

For the analysis of the rheological behaviour of Compritol®888-based nanoparticles, studies have been performed after seven days and three months of storage at room temperature, under a constant stress amplitude of 1 Pa. Tables XXV and XXVI depict the results collected for SLN and NLC dispersions, respectively.

Table XXV: Storage modulus (G'), loss modulus (G'') and complex viscosity (Eta) of aqueous Compritol®888-based SLN dispersions as a function of frequency, recorded after seven days (D7) and three months (M3) of storage at room temperature, under a constant stress amplitude of 1 Pa. (C888SLN_Ke^{dark} stands for SLN containing ketoconazole stored at 25ºC under light protection).

Sample	Storage time	f [Hz]	G' [Pa]	G'' [Pa]	Eta [mPa.s]
C888SLN	D7	1	4	2	756
		10	135	118	2860
	M3	1	322000	85700	53000000
		10	7460	177000	2820000
C888SLN_Ke	D7	1	2	1	422
		10	198	77	3380
	M3	1	4	3	740
		10	164	12	2610
C888SLN_Ke^{dark}	D7	1	2	2	406
		10	137	0	2336
	M3	1	5	6	1270
		10	302	145	5330

The aim of this study was the comparison of all viscoelastic parameters between the ones registered on day seven and those recorded after three months of storage at room temperature. From Table XXV it is clearly visible the influence of the storage conditions on aqueous Compritol®888-based SLN dispersions. The shelf life increased the magnitude of all viscoelastic parameters of the samples C888SLN and C888SLN_Ke^{dark}. The most consistent dispersion was the C888SLN due to the very high values recorded after three months at room temperature, which is a sign of instability. In addition, the drop of the storage modulus (G') (from 322000 Pa to 7460 Pa) was only observed for this formulation. However, despite of the greatest elasticity loss, C888SLN was still clearly the most elastic aqueous dispersion after three months of storage at 25ºC.

During this shelf life, the viscoelastic parameters slightly decreased for C888SLN_Ke. However, the elastic behaviour of these aqueous dispersions increased which can also be seen from the loss tangent values. In fact, after applying a frequency of 10 Hz, on day seven the tan δ was approximately 0.389 and it decreased to 0.073 after three months. The higher the loss tangent is the less elastic is the aqueous dispersion.

Table XXVI: Storage modulus (G'), loss modulus (G'') and complex viscosity (Eta) of aqueous Compritol®888-based NLC dispersions as a function of frequency, recorded after seven days (D7) and three months (M3) of storage at room temperature, under a constant stress amplitude of 1 Pa. (C888NLC_Ke^{dark} stands for NLC containing ketoconazole stored at 25ºC under light protection).

Sample	Storage time	f [Hz]	G' [Pa]	G'' [Pa]	Eta [mPa.s]
C888NLC	D7	1	1510	260	244000
		10	2750	205	43900
	M3	1	2440	355	392000
		10	3850	378	61500
C888NLC_Ke	D7	1	6	7	1450
		10	200	82	3430
	M3	1	920	298	154000
		10	2490	409	40200
C888NLC_Ke^{dark}	D7	1	3	1	344
		10	124	0	2033
	M3	1	2890	672	472000
		10	5590	534	89300

Regarding the aqueous Compritol®888-based NLC dispersions, Table XXVI also show the predominance of an elastic character (tan $\delta < 1$) of these formulations under different storage conditions. During shelf life, all viscoelastic parameters slightly increased comparing the values recorded on day seven and after three months for all aqueous dispersions. This first analysis shows that Compritol®888-based NLC dispersions are less unstable than Compritol®888-based SLN (Table XXV).

Analysing in detail the complex viscosity values it can also be concluded that Compritol®888-based NLC dispersions have a pseudoplastic-like behaviour after three months of storage at room temperature. In fact, the complex viscosity values decreased with the increase of the applied frequency range from 1 Hz to 10 Hz. Exceptions of this pattern were observed on day seven for the samples containing ketoconazole.